SCIENCE CHINA
Information Sciences

• RESEARCH PAPER •

April 2025, Vol. 68, Iss. 4, 142301:1–142301:17
https://doi.org/10.1007/s11432-024-4275-x

Two efficient beamforming methods for hybrid IRS-aided AF relay wireless networks

Xuehui WANG[1], Qingbo LI[1], Wen ZHU[2], Feng SHU[3,4,5*], Mengxing HUANG[3], Fuhui ZHOU[6], Riqing CHEN[7], Cunhua PAN[8], Yongpeng WU[9] & Jiangzhou WANG[10]

[1]*School of Mathematics and Statistics, Hainan Normal University, Haikou 571158, China*
[2]*Key Laboratory of Data Science and Smart Education, Ministry of Education, Hainan Normal University, Haikou 571158, China*
[3]*School of Information and Communication Engineering, Hainan University, Haikou 570228, China*
[4]*Collaborative Innovation Center of Information Technology, Hainan University, Haikou 570228, China*
[5]*School of Electronic and Optical Engineering, Nanjing University of Science and Technology, Nanjing 210094, China*
[6]*College of Electronic and Information Engineering, Nanjing University of Aeronautics and Astronautics, Nanjing 211106, China*
[7]*Digital Fujian Institute of Big Data for Agriculture, Fujian Agriculture and Forestry University, Fuzhou 350002, China*
[8]*National Mobile Communications Research Laboratory, Southeast University, Nanjing 211111, China*
[9]*Shanghai Key Laboratory of Navigation and Location Based Services, Shanghai Jiao Tong University, Shanghai 200240, China*
[10]*School of Engineering, University of Kent, Canterbury CT2 7NT, UK*

Received 5 March 2024/Revised 25 October 2024/Accepted 10 January 2025/Published online 20 February 2025

Abstract Owing to its ability to mitigate the double-fading effect by amplifying the reflected signal, the active intelligent reflecting surface (IRS) has garnered significant attention. In this paper, an amplify-and-forward (AF) relay network assisted by a hybrid IRS consisting of both passive and active units is developed. A signal-to-noise ratio (SNR) maximization problem is formulated, where the AF relay beamforming matrix and the hybrid IRS reflecting coefficient matrices for two-time slots need to be optimized. To address the SNR maximization problem, this paper proposes both a high-performance (HP) method and a low-complexity (LC) method. The HP method is based on the semidefinite relaxation and fractional programming (SDR-FP) algorithm, with rank-1 solutions obtained through Gaussian randomization. For the LC method, the amplification coefficient of each active IRS element is assumed to be equal. The SNR maximization problem is then addressed using the whitening filter, generalized power iteration, and generalized Rayleigh-Ritz (WF-GPI-GRR) approach. Simulation results show that compared with the benchmarks, such as the passive IRS-aided AF relay network, the proposed HP-SDR-FP and WF-GPI-GRR methods achieve significant rate improvements. In particular, the HP-SDR-FP and WF-GPI-GRR methods yield more than a 135.0% rate gain when the transmit power P_s of the source is 10 dBm. Furthermore, the proposed HP-SDR-FP method outperforms the WF-GPI-GRR method in terms of rate performance.

Keywords double-fading, intelligent reflecting surface, active elements, passive elements, hybrid IRS, AF relay

Citation Wang X H, Li Q B, Zhu W, et al. Two efficient beamforming methods for hybrid IRS-aided AF relay wireless networks. Sci China Inf Sci, 2025, 68(4): 142301, https://doi.org/10.1007/s11432-024-4275-x

1 Introduction

As information technologies rapidly advance, the Internet of Things (IoT) has made significant progress, while the number of smart devices in communication networks has grown exponentially [1]. Current technologies, such as wireless network coding, coordinated multipoint, millimeter-wave communication, and large-scale multiple-input multiple-output (MIMO), face challenges owing to high hardware overhead and energy consumption, making it difficult to meet the stringent requirements of high reliability, high data rates, and ultra-large-scale device interconnection [2–5]. In existing wireless networks, the cost of base stations (BSs) can be reduced, and the cooperation of multiple communication nodes can be enabled by deploying relay nodes, which helps achieve extended coverage and high reliability [6]. However, relays consume significant power to forward signals [7]. Therefore, it is essential to develop future wireless networks that are innovative, efficient, and resource-saving.

* Corresponding author (email: shufeng0101@163.com)

Owing to the advantages of low cost, easy deployment, and reconfigurability [8], both academia and industry have focused on research related to intelligent reflecting surfaces (IRS) [9]. An IRS consists of numerous passive electromagnetic units that can reflect incident signals to create an intelligent wireless propagation environment [10]. For IRS-aided communication networks, the authors in [11] introduced free-space channel models based on electromagnetic theory, radiation patterns, and physical principles. Additionally, an IRS-aided radio frequency (RF) system was proposed in [12], where the performance analyses of outage probability (OP) and bit error rate (BER) were presented. In [13], the authors proposed a single-input multiple-output wireless network aided by an IRS. The received signal power was enhanced by designing the IRS discrete phase shifts, while the optimal constellation was designed to maximize the minimum Euclidean distance using a novel modulation strategy; this approach avoided signal aliasing between the direct signal from the BS and the reflected signal from the IRS. Owing to its unique characteristics, the IRS is considered a promising technology for rate improvement and coverage extension. Currently, this technology is being extensively developed in various communication fields, including wireless-powered communication networks (WPCN) [14–16], multicell MIMO communications [17, 18], covert communications [19, 20], simultaneous wireless information and power transfer (SWIPT) [21,22], and physical layer security [23–25]. The authors in [16] considered a secure MIMO WPCN aided by an IRS and designed a joint optimization strategy for the transmit beamforming matrix, IRS phase shifts, energy transmit covariance matrix, and downlink/uplink time allocation, with the goal of maximizing the secrecy throughput for all users. In multicell communication systems [17], an IRS was deployed at the cell boundary. To achieve the maximum weighted sum rate, the beamforming matrices of the BSs and the IRS coefficient matrix were jointly optimized. In [25], the authors conducted a thorough study on a multiantenna system aided by an IRS, achieving the maximum secrecy rate by alternatively designing the source covariance and IRS reflecting matrix. Additionally, a simultaneously transmitting and reflecting (STAR)-IRS-aided SWIPT system was proposed in [26], where the BS transmit beamforming, the STAR-IRS transmission, and the reflection beamforming were optimized to maximize the weighted sum power.

Traditional relays have RF links, which enable strong signal processing capabilities such as decoding, amplification, and compression [27]. As a result, traditional relays are considered an effective strategy for improving rate and frequency efficiency [28]. In contrast, an IRS does not require complex RF chains or baseband circuits to reflect incident signals [29]. Since the IRS passively reflects the incident signal with extremely low power, it can be used as a green communication auxiliary technology [30]. To improve the rate performance of relay networks with low hardware overhead and power consumption, research on IRS-aided relay networks has been gaining increasing attention from researchers. Researchers have demonstrated that this combination can effectively serve wireless communication networks in terms of coverage extension [31, 32], rate performance [33, 34], spectral efficiency [35], and energy efficiency [36]. Using a decode-and-forward (DF) relaying protocol, an IRS-assisted dual-hop free-space optical and RF communication system was proposed in [31], where the exact closed-form expressions for OP and BER were derived. Simulation results verified that introducing an IRS could extend coverage. In [33], the authors proposed a DF relay wireless network aided by an IRS, which was designed with an iterative structure, null-space projection combined with maximum ratio combining (MRC), and IRS element selection with MRC methods to enhance rate performance. Additionally, it was shown that the combined network could achieve the same rate with fewer IRS elements compared with a network solely assisted by IRS [34].

However, the existing research mentioned earlier focuses on the conventional passive IRS. In reality, the reflected signal through the passive IRS is weak owing to the double-fading effect. To address this, recent studies have introduced an active IRS, which amplifies the reflected signal using additional power. In [37], the authors proposed the concept of the active IRS and developed an algorithm for jointly designing the transmit and reflect precoding to achieve maximum capacity; they also verified that the active IRS provides a significant capacity gain compared with the traditional passive one, demonstrating that the former can effectively eliminate the double-fading effect. In [38], the authors assumed that the overall power budgets were the same and provided a theoretical comparison of the performance between passive and active IRS. With an adequate power budget or small- to medium-sized IRS, the performance of the active IRS outperforms that of the passive one. Based on this, a novel active IRS-assisted secure wireless transmission system was proposed in [39], where a nonconvex problem of maximizing the secrecy rate was addressed by jointly optimizing the BS beamformer and IRS coefficient matrix. Compared with existing solutions, a significant secrecy rate gain was achieved with the assistance of active IRS. In addition, an active IRS-assisted multipair full-duplex communication network was investigated in [40],

where the performance under spatial correlation and imperfect channel state information was analyzed.

Given that active elements can mitigate the significant path loss associated with passive elements, the aim is to enhance the rate performance of passive IRS-aided amplify-and-forward (AF) relay networks and further improve communication quality. At the same time, the cost of the amplifier for active IRS elements and the need to reduce energy consumption to improve rate performance are considered. As a result, a hybrid IRS-assisted AF relay network is developed, where active elements are introduced alongside numerous passive elements to form the hybrid IRS. This combined network leverages the advantages of AF relay, passive IRS, and active IRS, balancing hardware costs, power consumption, and rate performance. According to the criterion of maximizing signal-to-noise ratio (SNR), two efficient methods are proposed to design the hybrid IRS reflecting coefficient matrices and the AF relay beamforming matrix, thereby maximizing the rate of the proposed AF relay wireless network aided by hybrid IRS. A summary of the contributions is presented as follows.

(1) To maximize the rate, a high-performance method based on the semidefinite relaxation and fractional programming (HP-SDR-FP) algorithm is introduced to jointly design the AF relay beamforming matrix and the hybrid IRS reflecting coefficient matrices by optimizing one variable at a time while fixing the others. However, directly tackling the nonconvex SNR maximization problem is challenging. Operations to overcome this, such as vectorization, Kronecker products, and Hadamard products, are applied to simplify the nonconvex optimization problem. The semidefinite relaxation (SDR) algorithm, Charnes-Cooper transformation (CCT) of the FP algorithm, and the Gaussian randomization method are then used to find the optimized variables. Compared with a passive IRS-aided AF relay network, the proposed HP-SDR-FP method achieves up to a 62.71% rate gain when the number of active IRS units, denoted by K, is 16; moreover, the HP-SDR-FP method converges quickly, although its computational complexity is relatively high.

(2) To reduce the computational complexity, the amplifying coefficient of each active IRS element is assumed to be the same in each time slot. According to the whitening filter, generalized power iteration algorithm, and generalized Rayleigh-Ritz theorem (WF-GPI-GRR), this paper proposes a low-complexity (LC) method. To fully exploit the colored nature of the noise, a whitening filter operation is applied to the received signal. In line with the transmit power at the AF relay and the power reflected by the hybrid IRS, the analytical solutions for the amplifying coefficients in both time slots are derived. Furthermore, the closed-form expression for the AF relay beamforming matrix is designed using the MRC and maximum-ratio transmission (MRC-MRT) scheme. The GPI algorithm and GRR are then applied to design the IRS phase shift matrices for the two-time slots. When $K = 16$, the rate is improved by 50.30% compared with that of a passive IRS-aided AF relay network.

The remaining chapters are organized as follows. In Section 2, the design of a novel AF relay network aided by a hybrid IRS is presented, and its optimization problem is formulated. Section 3 presents an HP method, whereas Section 4 introduces an LC method. Simulation results are provided in Section 5, and the corresponding conclusion is drawn in Section 6.

Notation. Lowercase, boldface lowercase, and boldface uppercase letters denote the scalars, vectors, and matrices, respectively. $(\cdot)^{-1}$, $(\cdot)^{\mathrm{T}}$, $(\cdot)^*$, and $(\cdot)^{\mathrm{H}}$ denote the inverse, transpose, conjugate, and conjugate transpose operations, respectively. $\mathrm{tr}(\cdot)$, $|\cdot|$, $\|\cdot\|$, $\|\cdot\|_F$, $\mathbb{E}\{\cdot\}$, and $\arg(\cdot)$ denote the operations for trace of a matrix, absolute value of a scalar, 2-norm, F-norm, expectation, and phase of a complex number, respectively. $\odot$ and $\otimes$ denote Hadamard and Kronecker products, respectively. $\boldsymbol{I}_N$ denotes the identity matrix of dimension N.

2 System model

Figure 1 shows a novel combination network called a hybrid IRS-aided AF relay network, where there is a barrier between single-antenna source (S) and single-antenna destination (D), the direct link from S to D is blocked. In this case, S can transmit data information to D with the aid of AF relay and hybrid IRS. The AF relay is with M antennas and works in half-duplex mode, and the hybrid IRS is made up of N units including K active units and L passive units. To reflect the incident signal, each active unit needs to adjust its amplifying coefficient and phase shift, while each passive unit only adjusts its phase.

The signs $\mathcal{E}_{\mathcal{N}}$, $\mathcal{E}_{\mathcal{K}}$, and $\mathcal{E}_{\mathcal{L}}$ are utilized to stand for the sets of N units, K active units, and L passive units, while their corresponding reflecting coefficient matrices can be represented as $\boldsymbol{\Theta}$, $\boldsymbol{\Phi}$, and $\boldsymbol{\Psi}$, respectively. Further, we have $\boldsymbol{\Theta} = \boldsymbol{\Phi} + \boldsymbol{\Psi}$, where $\boldsymbol{\Theta} = \mathrm{diag}(\alpha_1, \ldots, \alpha_N)$, $\boldsymbol{\Phi} = \mathrm{diag}(\phi_1, \ldots, \phi_N)$, and

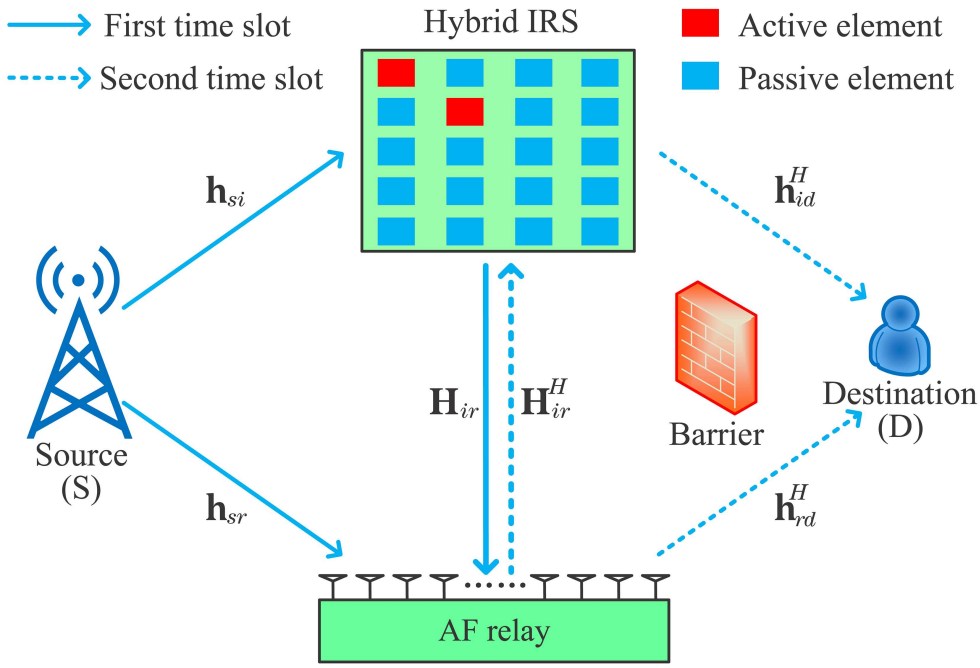

Figure 1 (Color online) AF relay network aided by hybrid IRS.

$\boldsymbol{\Psi} = \mathrm{diag}(\psi_1, \ldots, \psi_N)$. The ith reflecting coefficient in $\boldsymbol{\Theta}$, $\boldsymbol{\Phi}$, and $\boldsymbol{\Psi}$ is respectively denoted as

$$\alpha_i = \begin{cases} \beta_i \mathrm{e}^{\mathrm{j}\theta_i}, & i \in \mathcal{E}_{\mathcal{K}}, \quad (1a) \\ \mathrm{e}^{\mathrm{j}\theta_i}, & i \in \mathcal{E}_{\mathcal{L}}, \quad (1b) \end{cases}$$

$$\phi_i = \begin{cases} \beta_i \mathrm{e}^{\mathrm{j}\theta_i}, & i \in \mathcal{E}_{\mathcal{K}}, \quad (2a) \\ 0, & i \in \mathcal{E}_{\mathcal{L}}, \quad (2b) \end{cases}$$

$$\psi_i = \begin{cases} 0, & i \in \mathcal{E}_{\mathcal{K}}, \quad (3a) \\ \mathrm{e}^{\mathrm{j}\theta_i}, & i \in \mathcal{E}_{\mathcal{L}}, \quad (3b) \end{cases}$$

where $\beta_i \in \mathbb{R}_+$ denotes the amplifying coefficient and $\theta_i \in (0, 2\pi]$ is the phase shift of the ith unit.

For convenience, let us define

$$\boldsymbol{\Phi} = \boldsymbol{E}_K \boldsymbol{\Theta}, \quad \boldsymbol{\Psi} = \overline{\boldsymbol{E}}_K \boldsymbol{\Theta}, \tag{4}$$

where $\boldsymbol{E}_K \in \mathbb{R}^{N\times N}$ and $\overline{\boldsymbol{E}}_K \in \mathbb{R}^{N\times N}$ are diagonal matrices, which satisfy $\boldsymbol{E}_K \overline{\boldsymbol{E}}_K = \boldsymbol{0}_N$ and $\boldsymbol{E}_K + \overline{\boldsymbol{E}}_K = \boldsymbol{I}_N$. For $\boldsymbol{E}_K$, 0, and 1 on the diagonals are respectively corresponding to the passive and active units, while $\overline{\boldsymbol{E}}_K$ is opposite to $\boldsymbol{E}_K$. Furthermore, it is assumed that all links follow Rayleigh fading. $\boldsymbol{h}_{si} \in \mathbb{C}^{N\times 1}$, $\boldsymbol{H}_{ir} \in \mathbb{C}^{M\times N}$, $\boldsymbol{h}_{sr} \in \mathbb{C}^{M\times 1}$, $\boldsymbol{H}_{ir}^{\mathrm{H}} \in \mathbb{C}^{N\times M}$, $\boldsymbol{h}_{id}^{\mathrm{H}} \in \mathbb{C}^{1\times N}$, and $\boldsymbol{h}_{rd}^{\mathrm{H}} \in \mathbb{C}^{1\times M}$ respectively denote the channel responses of links S-IRS, IRS-AF relay, S-AF relay, AF relay-IRS, IRS-D, and AF relay-D. In the first time slot, let x satisfying $\mathbb{E}\{x^{\mathrm{H}}x\} = 1$ and P_s respectively denote the data symbol and the total power transmitted from S. The received signal at the hybrid IRS is given by

$$\boldsymbol{y}_{1i}^r = \sqrt{P_s}\boldsymbol{h}_{si}x + \boldsymbol{n}_{1i}, \tag{5}$$

where $\boldsymbol{n}_{1i}$ caused by active elements is the additive white Gaussian noise (AWGN), its distribution is $\boldsymbol{n}_{1i} \sim \mathcal{CN}(\boldsymbol{0}, \sigma_{1i}^2 \boldsymbol{E}_K \mathbf{I}_N)$. The received signal at the AF relay is expressed as

$$\begin{aligned} \boldsymbol{y}_r &= \sqrt{P_s}\boldsymbol{h}_{sr}x + \sqrt{P_s}\boldsymbol{H}_{ir}\boldsymbol{\Theta}_1\boldsymbol{h}_{si}x + \boldsymbol{H}_{ir}\boldsymbol{\Phi}_1\boldsymbol{n}_{1i} + \boldsymbol{n}_r \\ &= \sqrt{P_s}(\boldsymbol{h}_{sr} + \boldsymbol{H}_{ir}\boldsymbol{\Theta}_1\boldsymbol{h}_{si})x + \boldsymbol{H}_{ir}\boldsymbol{E}_K\boldsymbol{\Theta}_1\boldsymbol{n}_{1i} + \boldsymbol{n}_r, \end{aligned} \tag{6}$$

where $\boldsymbol{\Theta}_1 = \mathrm{diag}(\alpha_{11}, \ldots, \alpha_{1N})$ and $\boldsymbol{\Phi}_1 = \mathrm{diag}(\phi_{11}, \ldots, \phi_{1N})$ are the reflecting coefficient matrices corresponding to $\mathcal{E}_{\mathcal{N}}$ and $\mathcal{E}_{\mathcal{K}}$, and $\boldsymbol{n}_r \sim \mathcal{CN}(\boldsymbol{0}, \sigma_r^2 \boldsymbol{I}_M)$ is the AWGN at the AF relay.

In the second time slot, let $\boldsymbol{A} \in \mathbb{C}^{M\times M}$ stands for the AF relay beamforming matrix, and the signal transmitted from the AF relay is written by

$$\boldsymbol{y}_t = \boldsymbol{A}\boldsymbol{y}_r. \tag{7}$$

The signal reflected from the hybrid IRS is expressed as

$$\boldsymbol{y}_{2i}^t = \boldsymbol{\Theta}_2\boldsymbol{H}_{ir}^{\mathrm{H}}\boldsymbol{y}_t + \boldsymbol{\Phi}_2\boldsymbol{n}_{2i} = \boldsymbol{\Theta}_2\boldsymbol{H}_{ir}^{\mathrm{H}}\boldsymbol{y}_t + \boldsymbol{E}_K\boldsymbol{\Theta}_2\boldsymbol{n}_{2i}, \tag{8}$$

where $\boldsymbol{\Theta}_2 = \mathrm{diag}(\alpha_{21},\ldots,\alpha_{2N})$ and $\boldsymbol{\Phi}_2 = \mathrm{diag}(\phi_{21},\ldots,\phi_{2N})$ are the reflecting coefficient matrices corresponding to $\mathcal{E}_{\mathcal{N}}$ and $\mathcal{E}_{\mathcal{K}}$, and $\boldsymbol{n}_{2i} \sim \mathcal{CN}(\boldsymbol{0}, \sigma_{2i}^2\boldsymbol{E}_K\mathbf{I}_N)$ is the AWGN at the hybrid IRS. The received signal at D is given by

$$\begin{aligned} y_d =& \sqrt{P_s}(\boldsymbol{h}_{rd}^{\mathrm{H}} + \boldsymbol{h}_{id}^{\mathrm{H}}\boldsymbol{\Theta}_2\boldsymbol{H}_{ir}^{\mathrm{H}})\boldsymbol{A}(\boldsymbol{h}_{sr} + \boldsymbol{H}_{ir}\boldsymbol{\Theta}_1\boldsymbol{h}_{si})x \\ &+ (\boldsymbol{h}_{rd}^{\mathrm{H}} + \boldsymbol{h}_{id}^{\mathrm{H}}\boldsymbol{\Theta}_2\boldsymbol{H}_{ir}^{\mathrm{H}})\boldsymbol{A}(\boldsymbol{H}_{ir}\boldsymbol{E}_K\boldsymbol{\Theta}_1\boldsymbol{n}_{1i} + \boldsymbol{n}_r) + \boldsymbol{h}_{id}^{\mathrm{H}}\boldsymbol{E}_K\boldsymbol{\Theta}_2\boldsymbol{n}_{2i} + n_d, \end{aligned} \tag{9}$$

where $n_d \sim \mathcal{CN}(0,\sigma_d^2)$ is the AWGN. Let us define $\sigma_{1i}^2 = \sigma_{2i}^2 = \sigma_r^2 = \sigma_d^2 = \sigma^2$ and $\gamma_s = \frac{P_s}{\sigma^2}$, we have achievable system rate

$$R = \frac{1}{2}\log_2(1+\mathrm{SNR}), \tag{10}$$

where SNR is represented as

$$\mathrm{SNR} = \frac{\gamma_s|(\boldsymbol{h}_{rd}^{\mathrm{H}} + \boldsymbol{h}_{id}^{\mathrm{H}}\boldsymbol{\Theta}_2\boldsymbol{H}_{ir}^{\mathrm{H}})\boldsymbol{A}(\boldsymbol{h}_{sr} + \boldsymbol{H}_{ir}\boldsymbol{\Theta}_1\boldsymbol{h}_{si})|^2}{\|(\boldsymbol{h}_{rd}^{\mathrm{H}} + \boldsymbol{h}_{id}^{\mathrm{H}}\boldsymbol{\Theta}_2\boldsymbol{H}_{ir}^{\mathrm{H}})\boldsymbol{A}\boldsymbol{H}_{ir}\boldsymbol{E}_K\boldsymbol{\Theta}_1\|^2 + \|(\boldsymbol{h}_{rd}^{\mathrm{H}} + \boldsymbol{h}_{id}^{\mathrm{H}}\boldsymbol{\Theta}_2\boldsymbol{H}_{ir}^{\mathrm{H}})\boldsymbol{A}\|^2 + \|\boldsymbol{h}_{id}^{\mathrm{H}}\boldsymbol{E}_K\boldsymbol{\Theta}_2\|^2 + 1}. \tag{11}$$

It is similar to [33], all the channel state information is assumed to be available. Accordingly, the maximizing SNR problem is designed as follows:

$$\max_{\boldsymbol{A},\boldsymbol{\Theta}_1,\boldsymbol{\Theta}_2} \quad \mathrm{SNR} \tag{12a}$$

$$\text{s.t.} \quad |\boldsymbol{\Theta}_1(i,i)| = 1,\ |\boldsymbol{\Theta}_2(i,i)| = 1,\ \text{for } i \in \mathcal{E}_{\mathcal{L}}, \tag{12b}$$

$$\gamma_s\|\boldsymbol{E}_K\boldsymbol{\Theta}_1\boldsymbol{h}_{si}\|^2 + \|\boldsymbol{E}_K\boldsymbol{\Theta}_1\|_F^2 \leqslant \gamma_i, \tag{12c}$$

$$\gamma_s\|\boldsymbol{A}(\boldsymbol{h}_{sr} + \boldsymbol{H}_{ir}\boldsymbol{\Theta}_1\boldsymbol{h}_{si})\|^2 + \|\boldsymbol{A}\boldsymbol{H}_{ir}\boldsymbol{E}_K\boldsymbol{\Theta}_1\|_F^2 + \|\boldsymbol{A}\|_F^2 \leqslant \gamma_r, \tag{12d}$$

$$\begin{aligned} &\gamma_s\|\boldsymbol{E}_K\boldsymbol{\Theta}_2\boldsymbol{H}_{ir}^{\mathrm{H}}\boldsymbol{A}(\boldsymbol{h}_{sr} + \boldsymbol{H}_{ir}\boldsymbol{\Theta}_1\boldsymbol{h}_{si})\|^2 + \|\boldsymbol{E}_K\boldsymbol{\Theta}_2\boldsymbol{H}_{ir}^{\mathrm{H}}\boldsymbol{A}\boldsymbol{H}_{ir}\boldsymbol{E}_K\boldsymbol{\Theta}_1\|_F^2 \\ &+ \|\boldsymbol{E}_K\boldsymbol{\Theta}_2\boldsymbol{H}_{ir}^{\mathrm{H}}\boldsymbol{A}\|_F^2 + \|\boldsymbol{E}_K\boldsymbol{\Theta}_2\|_F^2 \leqslant \gamma_i, \end{aligned} \tag{12e}$$

where $\gamma_i = \frac{P_i}{\sigma^2}$ and $\gamma_r = \frac{P_r}{\sigma^2}$, wherein P_i and P_r are the transmit power budgets of the hybrid IRS and the AF relay. Since the IRS is a hybrid, solving the non-convex problem is a challenge in general. To achieve a maximum rate, two efficient beamforming methods called HP-SDR-FP and WF-GPI-GRR are proposed to optimize variables $\boldsymbol{A}$, $\boldsymbol{\Theta}_1$ and $\boldsymbol{\Theta}_2$.

3 Proposed HP-SDR-FP method

In this section, aiming to obtain maximum SNR, the HP-SDR-FP method is proposed, where the optimization problem (12) is decoupled into three subproblems by optimizing one and fixing the others. Each subproblem is firstly relaxed to an SDR problem, and which can be further transformed into a standard semidefinite programming (SDP) problem through the Charnes-Cooper transform of the FP algorithm. The SDP problem is convex and is solved by the CVX tool. In the relaxing process, the rank-1 constraint is ignored. So Gaussian randomization method is utilized to attain the rank-1 solution.

3.1 Optimization of $\boldsymbol{A}$ given $\boldsymbol{\Theta}_1$ and $\boldsymbol{\Theta}_2$

Given $\boldsymbol{\Theta}_1$ and $\boldsymbol{\Theta}_2$, the original problem (12) is reduced to

$$\max_{\boldsymbol{A}} \quad \mathrm{SNR} \tag{13a}$$

$$\text{s.t.} \quad (12\text{d}), \quad (12\text{e}). \tag{13b}$$

Let us define $\boldsymbol{a}=\mathrm{vec}(\boldsymbol{A})\in\mathbb{C}^{M^2\times 1}$, we have

$$\mathrm{SNR}=\frac{\gamma_s\boldsymbol{a}^{\mathrm{H}}\boldsymbol{B}_1\boldsymbol{a}}{\boldsymbol{a}^{\mathrm{H}}(\boldsymbol{B}_2+\boldsymbol{B}_3)\boldsymbol{a}+\|\boldsymbol{h}_{id}^{\mathrm{H}}\boldsymbol{E}_K\boldsymbol{\Theta}_2\|^2+1}, \tag{14}$$

where $\boldsymbol{B}_1=[(\boldsymbol{h}_{sr}+\boldsymbol{H}_{ir}\boldsymbol{\Theta}_1\boldsymbol{h}_{si})^*(\boldsymbol{h}_{sr}+\boldsymbol{H}_{ir}\boldsymbol{\Theta}_1\boldsymbol{h}_{si})^{\mathrm{T}}]\otimes[(\boldsymbol{h}_{rd}^{\mathrm{H}}+\boldsymbol{h}_{id}^{\mathrm{H}}\boldsymbol{\Theta}_2\boldsymbol{H}_{ir}^{\mathrm{H}})^{\mathrm{H}}(\boldsymbol{h}_{rd}^{\mathrm{H}}+\boldsymbol{h}_{id}^{\mathrm{H}}\boldsymbol{\Theta}_2\boldsymbol{H}_{ir}^{\mathrm{H}})]$, $\boldsymbol{B}_2=[(\boldsymbol{H}_{ir}\boldsymbol{E}_K\boldsymbol{\Theta}_1)^*(\boldsymbol{H}_{ir}\boldsymbol{E}_K\boldsymbol{\Theta}_1)^{\mathrm{T}}]\otimes[(\boldsymbol{h}_{rd}^{\mathrm{H}}+\boldsymbol{h}_{id}^{\mathrm{H}}\boldsymbol{\Theta}_2\boldsymbol{H}_{ir}^{\mathrm{H}})^{\mathrm{H}}(\boldsymbol{h}_{rd}^{\mathrm{H}}+\boldsymbol{h}_{id}^{\mathrm{H}}\boldsymbol{\Theta}_2\boldsymbol{H}_{ir}^{\mathrm{H}})]$ and $\boldsymbol{B}_3=\boldsymbol{I}_M\otimes[(\boldsymbol{h}_{rd}^{\mathrm{H}}+\boldsymbol{h}_{id}^{\mathrm{H}}\boldsymbol{\Theta}_2\boldsymbol{H}_{ir}^{\mathrm{H}})^{\mathrm{H}}\cdot(\boldsymbol{h}_{rd}^{\mathrm{H}}+\boldsymbol{h}_{id}^{\mathrm{H}}\boldsymbol{\Theta}_2\boldsymbol{H}_{ir}^{\mathrm{H}})]$. Similarly, the constraints (12d) and (12e) are translated to

$$\boldsymbol{a}^{\mathrm{H}}(\gamma_s\boldsymbol{C}_1+\boldsymbol{C}_2+\boldsymbol{I}_{M^2})\boldsymbol{a}\leqslant\gamma_r, \tag{15a}$$

$$\boldsymbol{a}^{\mathrm{H}}(\gamma_s\boldsymbol{D}_1+\boldsymbol{D}_2+\boldsymbol{D}_3)\boldsymbol{a}+\|\boldsymbol{E}_K\boldsymbol{\Theta}_2\|_F^2\leqslant\gamma_i, \tag{15b}$$

where $\boldsymbol{C}_1=[(\boldsymbol{h}_{sr}+\boldsymbol{H}_{ir}\boldsymbol{\Theta}_1\boldsymbol{h}_{si})^*(\boldsymbol{h}_{sr}+\boldsymbol{H}_{ir}\boldsymbol{\Theta}_1\boldsymbol{h}_{si})^{\mathrm{T}}]\otimes\boldsymbol{I}_M$, $\boldsymbol{C}_2=[(\boldsymbol{H}_{ir}\boldsymbol{E}_K\boldsymbol{\Theta}_1)^*(\boldsymbol{H}_{ir}\boldsymbol{E}_K\boldsymbol{\Theta}_1)^{\mathrm{T}}]\otimes\boldsymbol{I}_M$, $\boldsymbol{D}_1=[(\boldsymbol{h}_{sr}+\boldsymbol{H}_{ir}\boldsymbol{\Theta}_1\boldsymbol{h}_{si})^*(\boldsymbol{h}_{sr}+\boldsymbol{H}_{ir}\boldsymbol{\Theta}_1\boldsymbol{h}_{si})^{\mathrm{T}}]\otimes[(\boldsymbol{E}_K\boldsymbol{\Theta}_2\boldsymbol{H}_{ir}^{\mathrm{H}})^{\mathrm{H}}(\boldsymbol{E}_K\boldsymbol{\Theta}_2\boldsymbol{H}_{ir}^{\mathrm{H}})]$, $\boldsymbol{D}_2=[(\boldsymbol{H}_{ir}\boldsymbol{E}_K\boldsymbol{\Theta}_1)^*(\boldsymbol{H}_{ir}\boldsymbol{E}_K\boldsymbol{\Theta}_1)^{\mathrm{T}}]\otimes[(\boldsymbol{E}_K\boldsymbol{\Theta}_2\boldsymbol{H}_{ir}^{\mathrm{H}})^{\mathrm{H}}(\boldsymbol{E}_K\boldsymbol{\Theta}_2\boldsymbol{H}_{ir}^{\mathrm{H}})]$ and $\boldsymbol{D}_3=\boldsymbol{I}_M\otimes[(\boldsymbol{E}_K\boldsymbol{\Theta}_2\boldsymbol{H}_{ir}^{\mathrm{H}})^{\mathrm{H}}(\boldsymbol{E}_K\boldsymbol{\Theta}_2\boldsymbol{H}_{ir}^{\mathrm{H}})]$. Let us define $\widehat{\boldsymbol{A}}=\boldsymbol{a}\boldsymbol{a}^{\mathrm{H}}\in\mathbb{C}^{M^2\times M^2}$, the above problem is remodeled as

$$\max_{\widehat{\boldsymbol{A}}}\quad\frac{\gamma_s\mathrm{tr}(\boldsymbol{B}_1\widehat{\boldsymbol{A}})}{\mathrm{tr}\{(\boldsymbol{B}_2+\boldsymbol{B}_3)\widehat{\boldsymbol{A}}\}+\|\boldsymbol{h}_{id}^{\mathrm{H}}\boldsymbol{E}_K\boldsymbol{\Theta}_2\|^2+1} \tag{16a}$$

$$\text{s.t.}\quad\mathrm{tr}\{(\gamma_s\boldsymbol{C}_1+\boldsymbol{C}_2+\boldsymbol{I}_{M^2})\widehat{\boldsymbol{A}}\}\leqslant\gamma_r, \tag{16b}$$

$$\mathrm{tr}\{(\gamma_s\boldsymbol{D}_1+\boldsymbol{D}_2+\boldsymbol{D}_3)\widehat{\boldsymbol{A}}\}+\|\boldsymbol{E}_K\boldsymbol{\Theta}_2\|_F^2\leqslant\gamma_i, \tag{16c}$$

$$\widehat{\boldsymbol{A}}\succeq\boldsymbol{0},\quad\mathrm{rank}(\widehat{\boldsymbol{A}})=1, \tag{16d}$$

which is a non-convex problem because of the rank-one constraint. After removing $\mathrm{rank}(\widehat{\boldsymbol{A}})=1$ constraint, we have the following SDR problem:

$$\max_{\widehat{\boldsymbol{A}}}\quad\frac{\gamma_s\mathrm{tr}(\boldsymbol{B}_1\widehat{\boldsymbol{A}})}{\mathrm{tr}\{(\boldsymbol{B}_2+\boldsymbol{B}_3)\widehat{\boldsymbol{A}}\}+\|\boldsymbol{h}_{id}^{\mathrm{H}}\boldsymbol{E}_K\boldsymbol{\Theta}_2\|^2+1} \tag{17a}$$

$$\text{s.t.}\quad\text{(16b)},\quad\text{(16c)},\quad\widehat{\boldsymbol{A}}\succeq\boldsymbol{0}, \tag{17b}$$

which is quasi-convex because of the quasi-convex objective function and the convex constraints. It is necessary to apply CCT to convert the optimization problem from quasi-convex to convex. Introducing a slack variable m and defining $m=(\mathrm{tr}\{(\boldsymbol{B}_2+\boldsymbol{B}_3)\widehat{\boldsymbol{A}}\}+\|\boldsymbol{h}_{id}^{\mathrm{H}}\boldsymbol{E}_K\boldsymbol{\Theta}_2\|^2+1)^{-1}$, the above problem (17) is further rewritten as follows:

$$\max_{\widetilde{\boldsymbol{A}},m}\quad\gamma_s\mathrm{tr}\{\boldsymbol{B}_1\widetilde{\boldsymbol{A}}\} \tag{18a}$$

$$\text{s.t.}\quad\mathrm{tr}\{(\gamma_s\boldsymbol{C}_1+\boldsymbol{C}_2+\boldsymbol{I}_{M^2})\widetilde{\boldsymbol{A}}\}\leqslant m\gamma_r, \tag{18b}$$

$$\mathrm{tr}\{(\gamma_s\boldsymbol{D}_1+\boldsymbol{D}_2+\boldsymbol{D}_3)\widetilde{\boldsymbol{A}}\}+m\|\boldsymbol{E}_K\boldsymbol{\Theta}_2\|_F^2\leqslant m\gamma_i, \tag{18c}$$

$$\mathrm{tr}\{(\boldsymbol{B}_2+\boldsymbol{B}_3)\widetilde{\boldsymbol{A}}\}+m\|\boldsymbol{h}_{id}^{\mathrm{H}}\boldsymbol{E}_K\boldsymbol{\Theta}_2\|^2+m=1, \tag{18d}$$

$$\widetilde{\boldsymbol{A}}\succeq\boldsymbol{0},\ m>0, \tag{18e}$$

where $\widetilde{\boldsymbol{A}}=m\widehat{\boldsymbol{A}}$. Clearly, the above optimization problem has become an SDP problem, which is directly solved by CVX. The solution for problem (17) is $\widehat{\boldsymbol{A}}=\widetilde{\boldsymbol{A}}/m$. Since the constraint $\mathrm{rank}(\widehat{\boldsymbol{A}})=1$ is not considered in the SDR problem, the obtained solution $\widehat{\boldsymbol{A}}$ cannot meeting $\mathrm{rank}(\widehat{\boldsymbol{A}})=1$ in general. Here, the rank-one solution $\widehat{\boldsymbol{A}}$ is achieved via Gaussian randomization, thereby, $\boldsymbol{A}$ is attained.

3.2 Optimization of $\boldsymbol{\Theta}_1$ given $\boldsymbol{A}$ and $\boldsymbol{\Theta}_2$

Fixing $\boldsymbol{A}$ and $\boldsymbol{\Theta}_2$, problem (12) is reduced to

$$\max_{\boldsymbol{\Theta}_1}\quad\frac{\gamma_s|\boldsymbol{h}_{rid}^{\mathrm{H}}(\boldsymbol{h}_{sr}+\boldsymbol{H}_{ir}\boldsymbol{\Theta}_1\boldsymbol{h}_{si})|^2}{\|\boldsymbol{h}_{rid}^{\mathrm{H}}\boldsymbol{H}_{ir}\boldsymbol{E}_K\boldsymbol{\Theta}_1\|^2+\|\boldsymbol{h}_{rid}^{\mathrm{H}}\|^2+\|\boldsymbol{h}_{id}^{\mathrm{H}}\boldsymbol{E}_K\boldsymbol{\Theta}_2\|^2+1} \tag{19a}$$

$$\text{s.t.} \quad |\boldsymbol{\Theta}_1(i,i)| = 1, \quad \text{for } i \in \mathcal{E}_{\mathcal{L}}, \tag{19b}$$

$$(12c), \quad (12d), \quad (12e), \tag{19c}$$

where $\boldsymbol{h}_{rid} = [(\boldsymbol{h}_{rd}^{\mathrm{H}} + \boldsymbol{h}_{id}^{\mathrm{H}}\boldsymbol{\Theta}_2\boldsymbol{H}_{ir}^{\mathrm{H}})\boldsymbol{A}]^{\mathrm{H}}$. To further simplify the objective function and constraints, let us define $\boldsymbol{u}_1 = [\alpha_{11}, \ldots, \alpha_{1N}]^{\mathrm{T}}$, we have $\boldsymbol{h}_{sr} + \boldsymbol{H}_{ir}\boldsymbol{\Theta}_1\boldsymbol{h}_{si} = \boldsymbol{H}_{sir}\boldsymbol{v}_1$ and $\boldsymbol{h}_{rid}^{\mathrm{H}}\boldsymbol{H}_{ir}\boldsymbol{E}_K\boldsymbol{\Theta}_1 = \boldsymbol{u}_1^{\mathrm{T}}\mathrm{diag}\{\boldsymbol{h}_{rid}^{\mathrm{H}}\boldsymbol{H}_{ir}\boldsymbol{E}_K\}$, where $\boldsymbol{v}_1 = [\boldsymbol{u}_1; 1]$ and $\boldsymbol{H}_{sir} = [\boldsymbol{H}_{ir}\mathrm{diag}\{\boldsymbol{h}_{si}\}, \boldsymbol{h}_{sr}]$. Substituting these formulas into (19a), and due to the fact that $\|\boldsymbol{u}_1^{\mathrm{T}}\mathrm{diag}\{\boldsymbol{h}_{rid}^{\mathrm{H}}\boldsymbol{H}_{ir}\boldsymbol{E}_K\}\|^2 = \|\mathrm{diag}\{\boldsymbol{h}_{rid}^{\mathrm{H}}\boldsymbol{H}_{ir}\boldsymbol{E}_K\}\boldsymbol{u}_1\|^2$, the objective function is further rewritten as

$$\frac{\boldsymbol{v}_1^{\mathrm{H}}\boldsymbol{F}_1\boldsymbol{v}_1}{\boldsymbol{v}_1^{\mathrm{H}}\boldsymbol{F}_2\boldsymbol{v}_1}, \tag{20}$$

where $\boldsymbol{F}_1 = \gamma_s\boldsymbol{H}_{sir}^{\mathrm{H}}\boldsymbol{h}_{rid}\boldsymbol{h}_{rid}^{\mathrm{H}}\boldsymbol{H}_{sir}$ and $\boldsymbol{F}_2 = [\mathrm{diag}\{\boldsymbol{E}_K\boldsymbol{H}_{ir}^{\mathrm{H}}\boldsymbol{h}_{rid}\}\mathrm{diag}\{\boldsymbol{h}_{rid}^{\mathrm{H}}\boldsymbol{H}_{ir}\boldsymbol{E}_K\}, \boldsymbol{0}_{N\times 1}; \boldsymbol{0}_{1\times N}, \|\boldsymbol{h}_{rid}^{\mathrm{H}}\|^2 + \|\boldsymbol{h}_{id}^{\mathrm{H}}\boldsymbol{E}_K\boldsymbol{\Theta}_2\|^2 + 1]$. The constraint (19b) for passive elements $\mathcal{E}_{\mathcal{L}}$ is rewritten as

$$|\boldsymbol{v}_1(i)|^2 = 1, \quad \text{for } i \in \mathcal{E}_{\mathcal{L}}. \tag{21}$$

Obviously, $\|\boldsymbol{E}_K\boldsymbol{\Theta}_1\|_F^2 = \|\boldsymbol{E}_K\boldsymbol{u}_1\|^2$ and the constraint (12c) can be translated to

$$\boldsymbol{v}_1^{\mathrm{H}}\boldsymbol{G}_1\boldsymbol{v}_1 \leqslant \gamma_i, \tag{22}$$

where $\boldsymbol{G}_1 = [\gamma_s\mathrm{diag}\{\boldsymbol{h}_{si}^{\mathrm{H}}\}\boldsymbol{E}_K\mathrm{diag}\{\boldsymbol{h}_{si}\} + \boldsymbol{E}_K, \boldsymbol{0}_{N\times 1}; \boldsymbol{0}_{1\times N}, 0]$. Then for the constraint (12d), we have

$$\begin{aligned}
\|\boldsymbol{A}\boldsymbol{H}_{ir}\boldsymbol{E}_K\boldsymbol{\Theta}_1\|_F^2 &= \|\boldsymbol{A}\boldsymbol{H}_{ir}\boldsymbol{E}_K\mathrm{diag}\{\boldsymbol{u}_1\}\|_F^2 \\
&= \mathrm{tr}\{\boldsymbol{E}_K\boldsymbol{H}_{ir}^{\mathrm{H}}\boldsymbol{A}^{\mathrm{H}}\boldsymbol{A}\boldsymbol{H}_{ir}\boldsymbol{E}_K\mathrm{diag}\{\boldsymbol{u}_1\}\mathrm{diag}\{\boldsymbol{u}_1^{\mathrm{H}}\}\} \\
&= \mathrm{tr}\{\boldsymbol{E}_K\boldsymbol{H}_{ir}^{\mathrm{H}}\boldsymbol{A}^{\mathrm{H}}\boldsymbol{A}\boldsymbol{H}_{ir}[\boldsymbol{E}_K \odot (\boldsymbol{u}_1\boldsymbol{u}_1^{\mathrm{H}})]\} \\
&= \boldsymbol{u}_1^{\mathrm{H}}[(\boldsymbol{E}_K\boldsymbol{H}_{ir}^{\mathrm{H}}\boldsymbol{A}^{\mathrm{H}}\boldsymbol{A}\boldsymbol{H}_{ir}) \odot \boldsymbol{E}_K]\boldsymbol{u}_1 \\
&= \boldsymbol{u}_1^{\mathrm{H}}[(\boldsymbol{H}_{ir}^{\mathrm{H}}\boldsymbol{A}^{\mathrm{H}}\boldsymbol{A}\boldsymbol{H}_{ir}) \odot \boldsymbol{E}_K]\boldsymbol{u}_1.
\end{aligned} \tag{23}$$

Inserting $\boldsymbol{h}_{sr} + \boldsymbol{H}_{ir}\boldsymbol{\Theta}_1\boldsymbol{h}_{si} = \boldsymbol{H}_{sir}\boldsymbol{v}_1$ and (23) back into the constraint (12d), which is rewritten as

$$\boldsymbol{v}_1^{\mathrm{H}}\boldsymbol{G}_2\boldsymbol{v}_1 \leqslant \gamma_r, \tag{24}$$

where $\boldsymbol{G}_2 = \gamma_s\boldsymbol{H}_{sir}^{\mathrm{H}}\boldsymbol{A}^{\mathrm{H}}\boldsymbol{A}\boldsymbol{H}_{sir} + [(\boldsymbol{H}_{ir}^{\mathrm{H}}\boldsymbol{A}^{\mathrm{H}}\boldsymbol{A}\boldsymbol{H}_{ir}) \odot \boldsymbol{E}_K, \boldsymbol{0}_{N\times 1}; \boldsymbol{0}_{1\times N}, \|\boldsymbol{A}\|_F^2]$. Similarly, the constraint (12e) is converted to

$$\boldsymbol{v}_1^{\mathrm{H}}\boldsymbol{G}_3\boldsymbol{v}_1 \leqslant \gamma_i, \tag{25}$$

where $\boldsymbol{G}_3 = \gamma_s\boldsymbol{H}_{sir}^{\mathrm{H}}\boldsymbol{A}^{\mathrm{H}}\boldsymbol{H}_{ir}\boldsymbol{\Theta}_2^{\mathrm{H}}\boldsymbol{E}_K\boldsymbol{\Theta}_2\boldsymbol{H}_{ir}^{\mathrm{H}}\boldsymbol{A}\boldsymbol{H}_{sir} + [(\boldsymbol{H}_{ir}^{\mathrm{H}}\boldsymbol{A}^{\mathrm{H}}\boldsymbol{H}_{ir}\boldsymbol{\Theta}_2^{\mathrm{H}}\boldsymbol{E}_K\boldsymbol{\Theta}_2\boldsymbol{H}_{ir}^{\mathrm{H}}\boldsymbol{A}\boldsymbol{H}_{ir}) \odot \boldsymbol{E}_K, \boldsymbol{0}_{N\times 1}; \boldsymbol{0}_{1\times N}, \|\boldsymbol{E}_K\boldsymbol{\Theta}_2\boldsymbol{H}_{ir}^{\mathrm{H}}\boldsymbol{A}\|_F^2 + \|\boldsymbol{E}_K\boldsymbol{\Theta}_2\|_F^2]$. Substituting the simplified objective function and constraints into problem (19), which is equivalently transformed into

$$\max_{\boldsymbol{v}_1} \quad (20) \tag{26a}$$

$$\text{s.t.} \quad (21),\ (22),\ (24),\ (25),\ \boldsymbol{v}_1(N+1) = 1. \tag{26b}$$

Aiming at further transforming the optimization problem, defining $\boldsymbol{V}_1 = \boldsymbol{v}_1\boldsymbol{v}_1^{\mathrm{H}}$ and relaxing $\mathrm{rank}(\boldsymbol{V}_1) = 1$. After that, in the same manner, we define a slack variable $\tau = \mathrm{tr}(\boldsymbol{F}_2\boldsymbol{V}_1)^{-1}$ and $\widetilde{\boldsymbol{V}}_1 = \tau\boldsymbol{V}_1$. Problem (26) can be changed to the following SDP problem:

$$\max_{\widetilde{\boldsymbol{V}}_1, \tau} \quad \mathrm{tr}(\boldsymbol{F}_1\widetilde{\boldsymbol{V}}_1) \tag{27a}$$

$$\text{s.t.} \quad \widetilde{\boldsymbol{V}}_1(i,i) = \tau, \quad \text{for } i \in \mathcal{E}_{\mathcal{L}}, \tag{27b}$$

$$\widetilde{\boldsymbol{V}}_1(N+1, N+1) = \tau,\ \tau > 0, \tag{27c}$$

$$\mathrm{tr}(\boldsymbol{G}_1\widetilde{\boldsymbol{V}}_1) \leqslant \tau\gamma_i,\ \mathrm{tr}(\boldsymbol{G}_2\widetilde{\boldsymbol{V}}_1) \leqslant \tau\gamma_r, \tag{27d}$$

$$\mathrm{tr}(\boldsymbol{G}_3\widetilde{\boldsymbol{V}}_1) \leqslant \tau\gamma_i,\ \mathrm{tr}(\boldsymbol{F}_2\widetilde{\boldsymbol{V}}_1) = 1,\ \widetilde{\boldsymbol{V}}_1 \succeq \boldsymbol{0}. \tag{27e}$$

Its solution $\widetilde{\boldsymbol{V}}_1$ can be found via CVX tool, so that solution $\boldsymbol{V}_1$ is achieved, then a rank-one solution $\boldsymbol{V}_1$ is achieved through Gaussian randomization. Accordingly, the solution $\boldsymbol{v}_1$ is extracted from the eigenvalue

Algorithm 1 Proposed HP-SDR-FP method.

1. Given $(\boldsymbol{A}^0, \boldsymbol{\Theta}_1^0, \boldsymbol{\Theta}_2^0)$. According to (10), calculate R^0;
2. Set the convergence tolerance δ and the iterative number $t = 0$;
3. **repeat**
4. Given $(\boldsymbol{\Theta}_1^t, \boldsymbol{\Theta}_2^t)$, solve problem (18) for $\widehat{\boldsymbol{A}}^{t+1}$, recover rank-1 solution $\widehat{\boldsymbol{A}}^{t+1}$ via Gaussian randomization, obtain $\boldsymbol{A}^{t+1}$;
5. Given $(\boldsymbol{A}^{t+1}, \boldsymbol{\Theta}_2^t)$, solve problem (27) for $\widetilde{\boldsymbol{V}}_1^{t+1}$, recover rank-1 solution $\boldsymbol{V}_1^{t+1}$ via Gaussian randomization, obtain $\boldsymbol{\Theta}_1^{t+1}$;
6. Given $(\boldsymbol{A}^{t+1}, \boldsymbol{\Theta}_1^{t+1})$, solve problem (29) for $\widetilde{\boldsymbol{V}}_2^{t+1}$, recover rank-1 solution $\boldsymbol{V}_2^{t+1}$ via Gaussian randomization, obtain $\boldsymbol{\Theta}_2^{t+1}$;
7. Calculate R^{t+1} by using $(\boldsymbol{A}^{t+1}, \boldsymbol{\Theta}_1^{t+1}, \boldsymbol{\Theta}_2^{t+1})$;
8. Update $t = t + 1$;
9. **until**
   $|R^{t+1} - R^t| \leqslant \delta$.

decomposition of $\boldsymbol{V}_1$. Subsequently, the hybrid IRS reflecting coefficient matrix $\boldsymbol{\Theta}_1$ can be obtained as follows:

$$\boldsymbol{\Theta}_1(i,i) = \begin{cases} \mathrm{e}^{\mathrm{jarg}\left(\frac{\boldsymbol{v}_1(i)}{\boldsymbol{v}_1(N+1)}\right)}, & i \in \mathcal{E}_{\mathcal{L}}, \quad (28a) \\ \dfrac{\boldsymbol{v}_1(i)}{\boldsymbol{v}_1(N+1)}, & i \in \mathcal{E}_{\mathcal{K}}. \quad (28b) \end{cases}$$

3.3 Optimization of $\boldsymbol{\Theta}_2$ given $\boldsymbol{A}$ and $\boldsymbol{\Theta}_1$

When $\boldsymbol{A}$ and $\boldsymbol{\Theta}_1$ are fixed, the problem for $\boldsymbol{\Theta}_2$ is similar to that for $\boldsymbol{\Theta}_1$. In brief, we omit the related derivation process. In the same manner, we have

$$\begin{aligned} \max_{\widetilde{\boldsymbol{V}}_2, \rho} \quad & \mathrm{tr}(\boldsymbol{H}_1 \widetilde{\boldsymbol{V}}_2) && (29a) \\ \text{s.t.} \quad & \widetilde{\boldsymbol{V}}_2(i,i) = \rho, \ \text{ for } i \in \mathcal{E}_{\mathcal{L}}, && (29b) \\ & \widetilde{\boldsymbol{V}}_2(N+1, N+1) = \rho, \ \rho > 0, && (29c) \\ & \mathrm{tr}(\boldsymbol{J}\widetilde{\boldsymbol{V}}_2) \leqslant \rho\gamma_i, \ \mathrm{tr}(\boldsymbol{H}_2\widetilde{\boldsymbol{V}}_2) = 1, \ \widetilde{\boldsymbol{V}}_2 \succeq \boldsymbol{0}, && (29d) \end{aligned}$$

where matrices $\boldsymbol{H}_1 = \gamma_s \boldsymbol{H}_{rid}\boldsymbol{A}(\boldsymbol{h}_{sr} + \boldsymbol{H}_{ir}\boldsymbol{\Theta}_1\boldsymbol{h}_{si})[\boldsymbol{H}_{rid}\boldsymbol{A}(\boldsymbol{h}_{sr} + \boldsymbol{H}_{ir}\boldsymbol{\Theta}_1\boldsymbol{h}_{si})]^{\mathrm{H}}$, $\boldsymbol{H}_2 = \boldsymbol{H}_{rid}\boldsymbol{A}(\boldsymbol{H}_{ir}\boldsymbol{E}_K\boldsymbol{\Theta}_1\boldsymbol{\Theta}_1^{\mathrm{H}}\boldsymbol{E}_K\boldsymbol{H}_{ir}^{\mathrm{H}} + \boldsymbol{I}_M)\boldsymbol{A}^{\mathrm{H}}\boldsymbol{H}_{rid}^{\mathrm{H}} + \left[\mathrm{diag}\{\boldsymbol{h}_{id}^{\mathrm{H}}\boldsymbol{E}_K\}\mathrm{diag}\{\boldsymbol{E}_K\boldsymbol{h}_{id}\}, \ \boldsymbol{0}_{N\times 1}; \ \boldsymbol{0}_{1\times N}, \ 1\right]$ and $\boldsymbol{J} = [\gamma_s\boldsymbol{H}_3^{\mathrm{H}}\boldsymbol{H}_3 + (\boldsymbol{H}_4\boldsymbol{H}_4^{\mathrm{H}} + \boldsymbol{H}_{ir}^{\mathrm{H}}\boldsymbol{A}\boldsymbol{A}^{\mathrm{H}}\boldsymbol{H}_{ir} + \boldsymbol{I}_N)\odot\boldsymbol{E}_K, \ \boldsymbol{0}_{N\times 1}; \ \boldsymbol{0}_{1\times N}, \ 0]$, wherein $\boldsymbol{H}_3 = \boldsymbol{E}_K\mathrm{diag}\{\boldsymbol{H}_{ir}^{\mathrm{T}}\boldsymbol{A}^*(\boldsymbol{h}_{sr} + \boldsymbol{H}_{ir}\boldsymbol{\Theta}_1\boldsymbol{h}_{si})^*\}$ and $\boldsymbol{H}_4 = \boldsymbol{H}_{ir}^{\mathrm{H}}\boldsymbol{A}\boldsymbol{H}_{ir}\boldsymbol{E}_K\boldsymbol{\Theta}_1$. $\widetilde{\boldsymbol{V}}_2 = \rho\boldsymbol{v}_2\boldsymbol{v}_2^{\mathrm{H}}$, wherein $\boldsymbol{v}_2 = [\alpha_{21}, \ldots, \alpha_{2N}, 1]^{\mathrm{H}}$ and slack variable $\rho = \mathrm{tr}(\boldsymbol{H}_2\boldsymbol{v}_2\boldsymbol{v}_2^{\mathrm{H}})^{-1}$. Problem (29) can be solved in the same way as problem (27), and finally the solutions $\boldsymbol{v}_2$ and $\boldsymbol{\Theta}_2$ are obtained. The relationship between $\boldsymbol{\Theta}_2$ and $\boldsymbol{v}_2$ is as follows:

$$\boldsymbol{\Theta}_2(i,i) = \begin{cases} \mathrm{e}^{\mathrm{jarg}\left(\left[\frac{\boldsymbol{v}_2(i)}{\boldsymbol{v}_2(N+1)}\right]^*\right)}, & i \in \mathcal{E}_{\mathcal{L}}, \quad (30a) \\ \left[\dfrac{\boldsymbol{v}_2(i)}{\boldsymbol{v}_2(N+1)}\right]^*, & i \in \mathcal{E}_{\mathcal{K}}. \quad (30b) \end{cases}$$

3.4 Algorithm process and complexity calculation

Because of the non-decreasing objective function of problem (12) and the limit transmit powers of S, AF relay and IRS active elements, there exists an upper bound in the objective function. Therefore, the proposed HP-SDR-FP algorithm is convergent. Our idea is alternative iteration, that is, the alternative iteration process is performed among variables $\boldsymbol{A}$, $\boldsymbol{\Theta}_1$ and $\boldsymbol{\Theta}_2$, the system rate is maximum when the stopping requirement is satisfied. The process of the proposed HP-SDR-FP method is shown in Algorithm 1.

After that, the complexity of Algorithm 1 is calculated and analyzed according to problems (18), (27) and (29). Problem (18) has four 1-dimensional linear constraints, one linear matrix inequality (LMI) constraint with size M^2 and $M^4 + 1$ decision variables [41]. Hence, the computational complexity of problem (18) is given by

$$\mathcal{O}\{n_{\boldsymbol{A}}\sqrt{M^2+4}(M^6 + 4 + n_{\boldsymbol{A}}(M^4+4) + n_{\boldsymbol{A}}^2)\} \quad (31)$$

float-point operations (FLOPs), where $n_{\boldsymbol{A}} = M^4 + 1$. For problem (27), there exit $L + 6$ 1-dimensional linear constraints, one LMI constraint with size $N + 1$ and $(N + 1)^2 + 1$ decision variables. Consequently,

the computational complexity of problem (27) is represented as

$$\mathcal{O}\{n_{\boldsymbol{V}_1}\sqrt{N+L+7}((N+1)^3+L+6+n_{\boldsymbol{V}_1}((N+1)^2+L+6)+n_{\boldsymbol{V}_1}^2)\} \tag{32}$$

FLOPs, where $n_{\boldsymbol{V}_1}=(N+1)^2+1$. For problem (29), there are $L+4$ 1-dimensional linear constraints, one LMI constraint with size $N+1$ and $(N+1)^2+1$ decision variables. Thus the computational complexity of problem (29) is denoted as

$$\mathcal{O}\{n_{\boldsymbol{V}_2}\sqrt{N+L+5}((N+1)^3+L+4+n_{\boldsymbol{V}_2}((N+1)^2+L+4)+n_{\boldsymbol{V}_2}^2)\} \tag{33}$$

FLOPs, where $n_{\boldsymbol{V}_2}=(N+1)^2+1$. Consequently, the total computational complexity of the proposed HP-SDR-FP method is written by

$$\begin{aligned}&\mathcal{O}\{D_1[n_{\boldsymbol{A}}\sqrt{M^2+4}(M^6+4+n_{\boldsymbol{A}}(M^4+4)+n_{\boldsymbol{A}}^2)+n_{\boldsymbol{V}_1}\sqrt{N+L+7}((N+1)^3+L+6+n_{\boldsymbol{V}_1}((N+1)^2\\&+L+6)+n_{\boldsymbol{V}_1}^2)+n_{\boldsymbol{V}_2}\sqrt{N+L+5}((N+1)^3+L+4+n_{\boldsymbol{V}_2}((N+1)^2+L+4)+n_{\boldsymbol{V}_2}^2)]\}\end{aligned} \tag{34}$$

FLOPs, where D_1 is the maximum number of iterations required for convergence in Algorithm 1.

4 Proposed WF-GPI-GRR method

Since the optimization variables of the HP-SDR-FP method are matrices, which leads to extremely high computational complexity. Here, to reduce the computational complexity, an LC method based on WF, GPI and GRR is proposed, where active elements with equal gain reflect signal. In other words, the amplifying factors of active units for each time slot are individually equal. For convenience, variables $\boldsymbol{\Theta}_1$ and $\boldsymbol{\Theta}_2$ are respectively denoted as product forms related to the amplifying factor and the phase shift matrix. With the aim of obtaining rate improvement, WF operation is applied to exploit the colored property of noise, then the corresponding system model is presented. The derivations of the amplifying coefficient and the IRS phase shift matrix in each time slot and the AF relay beamforming matrix are described as follows.

4.1 System model

Defining the amplifying coefficient of each IRS active unit is β_1 for the first time slot and β_2 for the second time slot, we have

$$\boldsymbol{\Psi}_1=\overline{\boldsymbol{E}}_K\widehat{\boldsymbol{\Theta}}_1,\ \boldsymbol{\Phi}_1=\beta_1\boldsymbol{E}_K\widehat{\boldsymbol{\Theta}}_1, \tag{35a}$$

$$\boldsymbol{\Psi}_2=\overline{\boldsymbol{E}}_K\widehat{\boldsymbol{\Theta}}_2,\ \boldsymbol{\Phi}_2=\beta_2\boldsymbol{E}_K\widehat{\boldsymbol{\Theta}}_2, \tag{35b}$$

where the phase shift matrices $\widehat{\boldsymbol{\Theta}}_1=\mathrm{diag}(\mathrm{e}^{\mathrm{j}\theta_{1i}},\ldots,\mathrm{e}^{\mathrm{j}\theta_{1N}})$, $\widehat{\boldsymbol{\Theta}}_2=\mathrm{diag}(\mathrm{e}^{\mathrm{j}\theta_{2i}},\ldots,\mathrm{e}^{\mathrm{j}\theta_{2N}})$, $|\widehat{\boldsymbol{\Theta}}_1(i,i)|=1$, and $|\widehat{\boldsymbol{\Theta}}_2(i,i)|=1$. Then the reflecting coefficient matrices $\boldsymbol{\Theta}_1$ and $\boldsymbol{\Theta}_2$ are rewritten as

$$\boldsymbol{\Theta}_1=(\overline{\boldsymbol{E}}_K+\beta_1\boldsymbol{E}_K)\widehat{\boldsymbol{\Theta}}_1,\ \boldsymbol{\Theta}_2=(\overline{\boldsymbol{E}}_K+\beta_2\boldsymbol{E}_K)\widehat{\boldsymbol{\Theta}}_2. \tag{36}$$

In the first time slot, the received signal at the AF relay is

$$\boldsymbol{y}_r=\sqrt{P_s}[\boldsymbol{h}_{sr}+\boldsymbol{H}_{ir}(\overline{\boldsymbol{E}}_K+\beta_1\boldsymbol{E}_K)\widehat{\boldsymbol{\Theta}}_1\boldsymbol{h}_{si}]x+\underbrace{(\beta_1\boldsymbol{H}_{ir}\boldsymbol{E}_K\widehat{\boldsymbol{\Theta}}_1\boldsymbol{n}_{1i}+\boldsymbol{n}_r)}_{\boldsymbol{n}_{1r}}. \tag{37}$$

Since $\boldsymbol{n}_{1r}$ is colored not white, it is necessary for us to whiten the color noise $\boldsymbol{n}_{1r}$ by using covariance matrix $\boldsymbol{C}_{1r}$. The covariance W_{1r} of $\boldsymbol{n}_{1r}$ is given by

$$W_{1r}=\beta_1^2\|\boldsymbol{H}_{ir}\boldsymbol{E}_K\widehat{\boldsymbol{\Theta}}_1\|_F^2\sigma^2+\sigma^2. \tag{38}$$

$\boldsymbol{n}_{1i}$ and $\boldsymbol{n}_r$ are independent and identically distributed, thus $\boldsymbol{n}_{1r}$ has a mean vector of all-zeros and covariance matrix

$$\boldsymbol{C}_{1r}=\beta_1^2\sigma^2\boldsymbol{H}_{ir}\boldsymbol{E}_K\widehat{\boldsymbol{\Theta}}_1\widehat{\boldsymbol{\Theta}}_1^{\mathrm{H}}\boldsymbol{E}_K\boldsymbol{H}_{ir}^{\mathrm{H}}+\sigma^2\mathbf{I}_M, \tag{39}$$

where obviously $\boldsymbol{C}_{1r}$ is a positive definite matrix. Define the WF matrix $\boldsymbol{W}_{1r}$ with $\boldsymbol{W}_{1r}\boldsymbol{W}_{1r}^{\mathrm{H}} = \boldsymbol{C}_{1r}^{-1}$, which yields

$$\boldsymbol{W}_{1r} = \boldsymbol{C}_{1r}^{-\frac{1}{2}} = (\boldsymbol{Q}_{1r}\boldsymbol{\Lambda}_{1r}\boldsymbol{Q}_{1r}^{\mathrm{H}})^{-\frac{1}{2}} = \boldsymbol{Q}_{1r}\boldsymbol{\Lambda}_{1r}^{-\frac{1}{2}}\boldsymbol{Q}_{1r}^{\mathrm{H}}, \tag{40}$$

where $\boldsymbol{Q}_{1r}$ is an unitary matrix and $\boldsymbol{\Lambda}_{1r}$ is a diagonal matrix consisting of eigenvalues. Performing the WF operation to (37) yields

$$\overline{\boldsymbol{y}}_r = \sqrt{P_s}\boldsymbol{W}_{1r}[\boldsymbol{h}_{sr} + \boldsymbol{H}_{ir}(\overline{\boldsymbol{E}}_K + \beta_1\boldsymbol{E}_K)\widehat{\boldsymbol{\Theta}}_1\boldsymbol{h}_{si}]x + \underbrace{\boldsymbol{W}_{1r}(\beta_1\boldsymbol{H}_{ir}\boldsymbol{E}_K\widehat{\boldsymbol{\Theta}}_1\boldsymbol{n}_{1i} + \boldsymbol{n}_r)}_{\overline{\boldsymbol{n}}_{1r}}, \tag{41}$$

where $\overline{\boldsymbol{n}}_{1r}$ is the standard white noise with covariance matrix $\boldsymbol{I}_M$. The signal transmitted by the AF relay is $\overline{\boldsymbol{y}}_t = \boldsymbol{A}\overline{\boldsymbol{y}}_r$. In the second time slot, the received signal at D is denoted as

$$\begin{aligned} y_d = {} & \sqrt{P_s}[\boldsymbol{h}_{rd}^{\mathrm{H}} + \boldsymbol{h}_{id}^{\mathrm{H}}(\overline{\boldsymbol{E}}_K + \beta_2\boldsymbol{E}_K)\widehat{\boldsymbol{\Theta}}_2\boldsymbol{H}_{ir}^{\mathrm{H}}]\boldsymbol{A}\boldsymbol{W}_{1r}[\boldsymbol{h}_{sr} + \boldsymbol{H}_{ir}(\overline{\boldsymbol{E}}_K + \beta_1\boldsymbol{E}_K)\widehat{\boldsymbol{\Theta}}_1\boldsymbol{h}_{si}]x \\ & + [\boldsymbol{h}_{rd}^{\mathrm{H}} + \boldsymbol{h}_{id}^{\mathrm{H}}(\overline{\boldsymbol{E}}_K + \beta_2\boldsymbol{E}_K)\widehat{\boldsymbol{\Theta}}_2\boldsymbol{H}_{ir}^{\mathrm{H}}]\boldsymbol{A}\overline{\boldsymbol{n}}_{1r} + \beta_2\boldsymbol{h}_{id}^{\mathrm{H}}\boldsymbol{E}_K\widehat{\boldsymbol{\Theta}}_2\boldsymbol{n}_{2i} + n_d. \end{aligned} \tag{42}$$

The corresponding SNR can be represented as

$$\mathrm{SNR} = \frac{P_d}{N_d}, \tag{43}$$

where $P_d = \gamma_s|[\boldsymbol{h}_{rd}^{\mathrm{H}}+\boldsymbol{h}_{id}^{\mathrm{H}}(\overline{\boldsymbol{E}}_K+\beta_2\boldsymbol{E}_K)\widehat{\boldsymbol{\Theta}}_2\boldsymbol{H}_{ir}^{\mathrm{H}}]\boldsymbol{A}\boldsymbol{W}_{1r}[\boldsymbol{h}_{sr}+\boldsymbol{H}_{ir}(\overline{\boldsymbol{E}}_K+\beta_1\boldsymbol{E}_K)\widehat{\boldsymbol{\Theta}}_1\boldsymbol{h}_{si}]|^2$ and $N_d = \beta_1^2\|[\boldsymbol{h}_{rd}^{\mathrm{H}}+\boldsymbol{h}_{id}^{\mathrm{H}}(\overline{\boldsymbol{E}}_K+\beta_2\boldsymbol{E}_K)\widehat{\boldsymbol{\Theta}}_2\boldsymbol{H}_{ir}^{\mathrm{H}}]\boldsymbol{A}\boldsymbol{W}_{1r}\boldsymbol{H}_{ir}\boldsymbol{E}_K\widehat{\boldsymbol{\Theta}}_1\|^2+\|[\boldsymbol{h}_{rd}^{\mathrm{H}}+\boldsymbol{h}_{id}^{\mathrm{H}}(\overline{\boldsymbol{E}}_K+\beta_2\boldsymbol{E}_K)\widehat{\boldsymbol{\Theta}}_2\boldsymbol{H}_{ir}^{\mathrm{H}}]\boldsymbol{A}\boldsymbol{W}_{1r}\|^2+\beta_2^2\|\boldsymbol{h}_{id}^{\mathrm{H}}\boldsymbol{E}_K\widehat{\boldsymbol{\Theta}}_2\|^2+1$. It is assumed that the power budgets P_s, P_r, and P_i are respectively fully used to transmit signals at S, the AF relay and the hybrid IRS, the corresponding optimization problem is modeled as

$$\max_{\beta_1,\beta_2,\widehat{\boldsymbol{\Theta}}_1,\widehat{\boldsymbol{\Theta}}_2,\boldsymbol{A}} \quad (43) \tag{44a}$$

$$\text{s.t.} \quad |\widehat{\boldsymbol{\Theta}}_1(i,i)| = 1, \quad |\widehat{\boldsymbol{\Theta}}_2(i,i)| = 1. \tag{44b}$$

It is necessary to solve the above problem for optimal β_1, β_2, $\widehat{\boldsymbol{\Theta}}_1$, $\widehat{\boldsymbol{\Theta}}_2$, and $\boldsymbol{A}$.

4.2 Solve $\boldsymbol{\beta_1}$ and $\boldsymbol{\beta_2}$

In the first time slot, the signal reflected by the hybrid IRS is represented as

$$\boldsymbol{y}_{1i}^t = \sqrt{P_s}\boldsymbol{\Theta}_1\boldsymbol{h}_{si}x + \boldsymbol{\Phi}_1\boldsymbol{n}_{1i} = \underbrace{\sqrt{P_s}\overline{\boldsymbol{E}}_K\widehat{\boldsymbol{\Theta}}_1\boldsymbol{h}_{si}x}_{\boldsymbol{y}_{1i}^{pt}} + \underbrace{\sqrt{P_s}\beta_1\boldsymbol{E}_K\widehat{\boldsymbol{\Theta}}_1\boldsymbol{h}_{si}x + \beta_1\boldsymbol{E}_K\widehat{\boldsymbol{\Theta}}_1\boldsymbol{n}_{1i}}_{\boldsymbol{y}_{1i}^{at}}, \tag{45}$$

where $\boldsymbol{y}_{1i}^{pt}$ and $\boldsymbol{y}_{1i}^{at}$ are respectively the signals reflected by the passive elements $\mathcal{E}_{\mathcal{L}}$ and the active elements $\mathcal{E}_{\mathcal{K}}$. Additionally, the power P_i reflected by $\mathcal{E}_{\mathcal{K}}$ is

$$\begin{aligned} P_i &= P_s\beta_1^2\|\boldsymbol{E}_K\widehat{\boldsymbol{\Theta}}_1\boldsymbol{h}_{si}\|^2 + \beta_1^2\|\boldsymbol{E}_K\widehat{\boldsymbol{\Theta}}_1\|_F^2\sigma_{1i}^2 \\ &= \beta_1^2P_s\sum_{k=1}^{K}|\mathrm{e}^{\mathrm{j}\theta_{1k}}h_{si}^k|^2 + \beta_1^2\sum_{k=1}^{K}|\mathrm{e}^{\mathrm{j}\theta_{1k}}|^2\sigma_{1i}^2 \\ &= \beta_1^2P_s\sum_{k=1}^{K}|h_{si}^k|^2 + K\beta_1^2\sigma^2, \end{aligned} \tag{46}$$

where θ_{1k} stands for the phase shift corresponding to the kth IRS active element, h_{si}^k stands for the channel from S to the kth IRS active unit and follows Rayleigh distribution with the following expression:

$$h_{si}^k = \sqrt{\mathrm{PL}_{si}^k}g_{si}^k\mathrm{e}^{-\mathrm{j}\varphi_{sk}}, \tag{47}$$

where PL_{si}^k, g_{si}^k, and φ_{sk} denote the path loss, the channel gain, and the channel phase, respectively. $|g_{si}^k|^2$ follows exponential distribution [42], and the corresponding probability density function is given by

$$f_{|g_{si}^k|^2}(x) = \begin{cases} \lambda_{si}\mathrm{e}^{-\lambda_{si}x}, & x \in [0,+\infty), \quad (48a) \\ 0, & \text{otherwise}, \quad (48b) \end{cases}$$

where λ_{si} is the rate parameter. Let $\mathrm{PL}_{si}^{k}=\mathrm{PL}_{si}$, where PL_{si} is the path loss of $\boldsymbol{h}_{si}$. By utilizing the weak law of large numbers, Eq. (46) is further written as

$$\begin{aligned}P_i&=\beta_1^2P_s\sum_{k=1}^{K}|\sqrt{\mathrm{PL}_{si}}g_{si}^{k}\mathrm{e}^{-\mathrm{j}\varphi_{sk}}|^2+K\beta_1^2\sigma^2\\&=\beta_1^2P_s\mathrm{PL}_{si}\sum_{k=1}^{K}|g_{si}^{k}|^2+K\beta_1^2\sigma^2\\&\approx K\beta_1^2P_s\mathrm{PL}_{si}\cdot\mathbb{E}(|g_{si}^{k}|^2)+K\beta_1^2\sigma^2\\&=\frac{K\beta_1^2P_s\mathrm{PL}_{si}}{\lambda_{si}}+K\beta_1^2\sigma^2,\end{aligned}\tag{49}$$

where β_1 is achieved as

$$\beta_1=\sqrt{\frac{P_i\lambda_{si}}{KP_s\mathrm{PL}_{si}+K\lambda_{si}\sigma^2}}.\tag{50}$$

In the second time slot, the received signal of the kth active IRS element is similarly denoted as

$$y_{2i}^{rk}=\boldsymbol{h}_{rk}^{\mathrm{H}}\overline{\boldsymbol{y}}_t+n_{2i,k},\tag{51}$$

where $\boldsymbol{h}_{rk}^{\mathrm{H}}\in\mathbb{C}^{1\times M}$ represents the link from the AF relay to the kth active IRS unit.

$$\boldsymbol{h}_{rk}^{\mathrm{H}}=\left[\sqrt{\mathrm{PL}_{ri}^{1k}}g_{ri}^{1k}\mathrm{e}^{-\mathrm{j}\varphi_{1k}},\ldots,\sqrt{\mathrm{PL}_{ri}^{Mk}}g_{ri}^{Mk}\mathrm{e}^{-\mathrm{j}\varphi_{Mk}}\right],\tag{52}$$

where PL_{ri}^{mk}, g_{ri}^{mk}, and φ_{mk} are the path loss, the channel gain and the link phase from the mth antenna of the AF relay to the kth active IRS unit. Defining $\mathrm{PL}_{ri}^{mk}=\mathrm{PL}_{ri}$, PL_{ri} is the path loss from AF relay to IRS. The reflected signal of the kth active IRS element is

$$\begin{aligned}y_{2i}^{tk}&=\beta_2\mathrm{e}^{\mathrm{j}\theta_{2k}}\boldsymbol{h}_{rk}^{\mathrm{H}}\overline{\boldsymbol{y}}_t+\beta_2\mathrm{e}^{\mathrm{j}\theta_{2k}}n_{2i,k}\\&=\beta_2|\boldsymbol{h}_{rk}^{\mathrm{H}}\overline{\boldsymbol{y}}_t|\mathrm{e}^{\mathrm{j}(\theta_{2k}+\varphi_{rkt})}+\beta_2\mathrm{e}^{\mathrm{j}\theta_{2k}}n_{2i,k}\\&=\beta_2|\boldsymbol{h}_{rk}^{\mathrm{H}}||\overline{\boldsymbol{y}}_t|\mathrm{e}^{\mathrm{j}(\theta_{2k}+\varphi_{rkt})}+\beta_2\mathrm{e}^{\mathrm{j}\theta_{2k}}n_{2i,k},\end{aligned}\tag{53}$$

where θ_{2k} is the phase shift corresponding to the kth IRS active unit, φ_{rkt} is the phase of $\boldsymbol{h}_{rk}^{\mathrm{H}}\overline{\boldsymbol{y}}_t$. The reflected power of the kth active IRS unit is represented as

$$\begin{aligned}P_{2i}^{tk}&=\beta_2^2|\boldsymbol{h}_{rk}^{\mathrm{H}}|^2|\overline{\boldsymbol{y}}_t|^2+\beta_2^2\sigma_{2i,k}^2\\&=\beta_2^2P_r\mathrm{PL}_{ri}\sum_{m=1}^{M}|g_{ri}^{mk}|^2+\frac{\beta_2^2\sigma^2}{K}\\&\approx M\beta_2^2P_r\mathrm{PL}_{ri}\cdot\mathbb{E}(|g_{ri}^{mk}|^2)+\frac{\beta_2^2\sigma^2}{K}\\&=\frac{M\beta_2^2P_r\mathrm{PL}_{ri}}{\lambda_{ri}}+\frac{\beta_2^2\sigma^2}{K},\end{aligned}\tag{54}$$

where $\sigma_{2i,k}^2=\sigma_{2i}^2/K=\sigma^2/K$ and λ_{ri} stands for the rate parameter. Thus the power reflected by $\mathcal{E}_{\mathcal{K}}$ is

$$P_i=\sum_{k=1}^{K}P_{2i}^{tk}=\frac{KM\beta_2^2P_r\mathrm{PL}_{ri}}{\lambda_{ri}}+\beta_2^2\sigma^2,\tag{55}$$

which yields

$$\beta_2=\sqrt{\frac{P_i\lambda_{ri}}{KMP_r\mathrm{PL}_{ri}+\lambda_{ri}\sigma^2}}.\tag{56}$$

Algorithm 2 GPI algorithm to compute phase-shift vector $\widehat{\boldsymbol{v}}_1$ with given $\boldsymbol{A}$ and $\widehat{\boldsymbol{\Theta}}_2$.

1. Given $\boldsymbol{A}$ and $\widehat{\boldsymbol{\Theta}}_2$, and initialize $\widehat{\boldsymbol{v}}_1^0$;
2. Set the tolerance factor ξ and the iterative number $t=0$;
3. **repeat**
4. Compute the function matrix $\boldsymbol{\Omega}(\widehat{\boldsymbol{v}}_1^t)$ and $\boldsymbol{\Xi}_1(\widehat{\boldsymbol{v}}_1^t)$;
5. Calculate $\boldsymbol{y}^t=\boldsymbol{\Xi}_1(\widehat{\boldsymbol{v}}_1^t)^{\dagger}\boldsymbol{\Omega}(\widehat{\boldsymbol{v}}_1^t)\widehat{\boldsymbol{v}}_1^t$;
6. Update $\widehat{\boldsymbol{v}}_1^{t+1}=\frac{\boldsymbol{y}^t}{\|\boldsymbol{y}^t\|}$;
7. Update $t=t+1$;
8. **until**
$\|\widehat{\boldsymbol{v}}_1^{t+1}-\widehat{\boldsymbol{v}}_1^t\|\leqslant\xi$.

4.3 Optimize $\boldsymbol{A}$ given $\widehat{\boldsymbol{\Theta}}_1$ and $\widehat{\boldsymbol{\Theta}}_2$

Aiming at maximizing the received signal power, the MRC-MRT method is applied to solve $\boldsymbol{A}$ as follows:

$$\boldsymbol{A}=A\underbrace{\frac{[\boldsymbol{h}_{rd}+\boldsymbol{H}_{ir}\widehat{\boldsymbol{\Theta}}_2^{\mathrm{H}}(\overline{\boldsymbol{E}}_K+\beta_2\boldsymbol{E}_K)\boldsymbol{h}_{id}]}{\|\boldsymbol{h}_{rd}^{\mathrm{H}}+\boldsymbol{h}_{id}^{\mathrm{H}}(\overline{\boldsymbol{E}}_K+\beta_2\boldsymbol{E}_K)\widehat{\boldsymbol{\Theta}}_2\boldsymbol{H}_{ir}^{\mathrm{H}}\|}\frac{[\boldsymbol{h}_{sr}+\boldsymbol{H}_{ir}(\overline{\boldsymbol{E}}_K+\beta_1\boldsymbol{E}_K)\widehat{\boldsymbol{\Theta}}_1\boldsymbol{h}_{si}]^{\mathrm{H}}\boldsymbol{W}_{1r}^{\mathrm{H}}}{\|\boldsymbol{W}_{1r}[\boldsymbol{h}_{sr}+\boldsymbol{H}_{ir}(\overline{\boldsymbol{E}}_K+\beta_1\boldsymbol{E}_K)\widehat{\boldsymbol{\Theta}}_1\boldsymbol{h}_{si}]\|}}_{\boldsymbol{\Upsilon}},\tag{57}$$

where A is the amplifying factor of the AF relay. Since the transmit power of the AF relay is P_r, we have

$$A=\sqrt{\frac{\gamma_r}{\gamma_s\|\boldsymbol{\Upsilon}\boldsymbol{W}_{1r}[\boldsymbol{h}_{sr}+\boldsymbol{H}_{ir}(\overline{\boldsymbol{E}}_K+\beta_1\boldsymbol{E}_K)\widehat{\boldsymbol{\Theta}}_1\boldsymbol{h}_{si}]\|^2+\beta_1^2\|\boldsymbol{\Upsilon}\boldsymbol{W}_{1r}\boldsymbol{H}_{ir}\boldsymbol{E}_K\widehat{\boldsymbol{\Theta}}_1\|_F^2+\|\boldsymbol{\Upsilon}\boldsymbol{W}_{1r}\|_F^2}}.\tag{58}$$

Inserting A back into (57), $\boldsymbol{A}$ can be obtained.

4.4 Optimize $\widehat{\boldsymbol{\Theta}}_1$ given $\boldsymbol{A}$ and $\widehat{\boldsymbol{\Theta}}_2$

By defining $\widehat{\boldsymbol{u}}_1=[\mathrm{e}^{\mathrm{j}\theta_{1i}},\ldots,\mathrm{e}^{\mathrm{j}\theta_{1N}}]^{\mathrm{T}}$, $\widehat{\boldsymbol{v}}_1=[\widehat{\boldsymbol{u}}_1;1]$ and $\widehat{\boldsymbol{H}}_{sir}=[\boldsymbol{H}_{ir}(\overline{\boldsymbol{E}}_K+\beta_1\boldsymbol{E}_K)\mathrm{diag}\{\boldsymbol{h}_{si}\},\boldsymbol{h}_{sr}]$. Fixing $\boldsymbol{A}$ and $\widehat{\boldsymbol{\Theta}}_2$, problem (44) is simplified as

$$\max_{\widehat{\boldsymbol{v}}_1}\quad\frac{\widehat{\boldsymbol{v}}_1^{\mathrm{H}}\widehat{\boldsymbol{F}}_1\widehat{\boldsymbol{v}}_1}{\widehat{\boldsymbol{v}}_1^{\mathrm{H}}\widehat{\boldsymbol{F}}_2\widehat{\boldsymbol{v}}_1}\tag{59a}$$

$$\text{s.t.}\quad|\widehat{\boldsymbol{v}}_1(i)|=1,\ \forall i=1,2,\ldots,N,\tag{59b}$$

$$\widehat{\boldsymbol{v}}_1(N+1)=1,\tag{59c}$$

where $\widehat{\boldsymbol{F}}_1$ is a Hermitian matrix and $\widehat{\boldsymbol{F}}_1=\gamma_s\widehat{\boldsymbol{H}}_{sir}^{\mathrm{H}}[(\boldsymbol{h}_{rd}^{\mathrm{H}}+\boldsymbol{h}_{id}^{\mathrm{H}}(\overline{\boldsymbol{E}}_K+\beta_2\boldsymbol{E}_K)\widehat{\boldsymbol{\Theta}}_2\boldsymbol{H}_{ir}^{\mathrm{H}})\boldsymbol{A}\boldsymbol{W}_{1r}]^{\mathrm{H}}[(\boldsymbol{h}_{rd}^{\mathrm{H}}+\boldsymbol{h}_{id}^{\mathrm{H}}(\overline{\boldsymbol{E}}_K+\beta_2\boldsymbol{E}_K)\widehat{\boldsymbol{\Theta}}_2\boldsymbol{H}_{ir}^{\mathrm{H}})\boldsymbol{A}\boldsymbol{W}_{1r}]\widehat{\boldsymbol{H}}_{sir}$. Meanwhile, $\widehat{\boldsymbol{F}}_2$ is a positive semi-definite Hermitian matrix and $\widehat{\boldsymbol{F}}_2=[\beta_1^2\mathrm{diag}\{\boldsymbol{E}_K\boldsymbol{H}_{ir}^{\mathrm{H}}\widehat{\boldsymbol{h}}_{rid}\}\mathrm{diag}\{\widehat{\boldsymbol{h}}_{rid}^{\mathrm{H}}\boldsymbol{H}_{ir}\boldsymbol{E}_K\},\ \boldsymbol{0}_{N\times1};\ \boldsymbol{0}_{1\times N},\ \|\widehat{\boldsymbol{h}}_{rid}^{\mathrm{H}}\|^2+\beta_2^2\|\boldsymbol{h}_{id}^{\mathrm{H}}\boldsymbol{E}_K\widehat{\boldsymbol{\Theta}}_2\|^2+1]$. Problem (59) is relaxed to

$$\max_{\widehat{\boldsymbol{v}}_1}\quad\frac{\widehat{\boldsymbol{v}}_1^{\mathrm{H}}\widehat{\boldsymbol{F}}_1\widehat{\boldsymbol{v}}_1}{\widehat{\boldsymbol{v}}_1^{\mathrm{H}}\widehat{\boldsymbol{F}}_2\widehat{\boldsymbol{v}}_1}\tag{60a}$$

$$\text{s.t.}\quad\|\widehat{\boldsymbol{v}}_1\|^2=N+1,\tag{60b}$$

which is constructed as

$$\max_{\widehat{\boldsymbol{v}}_1}\quad\frac{\widehat{\boldsymbol{v}}_1^{\mathrm{H}}\widehat{\boldsymbol{F}}_1\widehat{\boldsymbol{v}}_1}{\widehat{\boldsymbol{v}}_1^{\mathrm{H}}\widehat{\boldsymbol{F}}_2\widehat{\boldsymbol{v}}_1}\cdot\frac{\widehat{\boldsymbol{v}}_1^{\mathrm{H}}\boldsymbol{I}_{N+1}\widehat{\boldsymbol{v}}_1}{\widehat{\boldsymbol{v}}_1^{\mathrm{H}}\boldsymbol{I}_{N+1}\widehat{\boldsymbol{v}}_1}\tag{61a}$$

$$\text{s.t.}\quad\|\widehat{\boldsymbol{v}}_1\|^2=N+1.\tag{61b}$$

$\widehat{\boldsymbol{v}}_1$ can be solved by the GPI algorithm, the details of the GPI procedure are presented in Algorithm 2, where we define $\boldsymbol{\Omega}(\widehat{\boldsymbol{v}}_1^t)=(\widehat{\boldsymbol{v}}_1^{\mathrm{H}}\widehat{\boldsymbol{F}}_1\widehat{\boldsymbol{v}}_1)\boldsymbol{I}_{N+1}+(\widehat{\boldsymbol{v}}_1^{\mathrm{H}}\boldsymbol{I}_{N+1}\widehat{\boldsymbol{v}}_1)\widehat{\boldsymbol{F}}_1$ and $\boldsymbol{\Xi}_1(\widehat{\boldsymbol{v}}_1^t)=(\widehat{\boldsymbol{v}}_1^{\mathrm{H}}\widehat{\boldsymbol{F}}_2\widehat{\boldsymbol{v}}_1)\boldsymbol{I}_{N+1}+(\widehat{\boldsymbol{v}}_1^{\mathrm{H}}\boldsymbol{I}_{N+1}\widehat{\boldsymbol{v}}_1)\widehat{\boldsymbol{F}}_2$.

Algorithm 3 Proposed WF-GPI-GRR method.

1. Calculate β_1 and β_2 through (50) and (56);
2. Initialize $\boldsymbol{A}^0$, $\widehat{\boldsymbol{\Theta}}_1^0$ and $\widehat{\boldsymbol{\Theta}}_2^0$. According to (10) and (43), obtain R^0;
3. Set the iterative number $t=0$ and the convergence accuracy δ;
4. **repeat**
5. Fix $\widehat{\boldsymbol{\Theta}}_1^t$ and $\widehat{\boldsymbol{\Theta}}_2^t$, obtain $\boldsymbol{A}^{t+1}$ through (57);
6. Fix $\boldsymbol{A}^{t+1}$ and $\widehat{\boldsymbol{\Theta}}_2^t$, obtain $\widehat{\boldsymbol{v}}_1^{t+1}$ by solving problem (61), $\widehat{\boldsymbol{\Theta}}_1^{t+1}=\mathrm{diag}\{\widehat{\boldsymbol{v}}_1^{t+1}(1:N)\}$;
7. Fix $\boldsymbol{A}^{t+1}$ and $\widehat{\boldsymbol{\Theta}}_1^{t+1}$, obtain $\widehat{\boldsymbol{v}}_2^{t+1}$ by solving problem (63), $\widehat{\boldsymbol{\Theta}}_2^{t+1}=\mathrm{diag}\{\widehat{\boldsymbol{v}}_2^{t+1}(1:N)\}$;
8. Obtain R^{t+1} by using β_1, β_2, $\boldsymbol{A}^{t+1}$, $\widehat{\boldsymbol{\Theta}}_1^{t+1}$ and $\widehat{\boldsymbol{\Theta}}_2^{t+1}$;
9. Let $t=t+1$;
10. **until**
$\left|R^{t+1}-R^t\right|\leqslant\delta$.

4.5 Optimize $\widehat{\boldsymbol{\Theta}}_2$ given $\boldsymbol{A}$ and $\widehat{\boldsymbol{\Theta}}_1$

Given $\boldsymbol{A}$ and $\widehat{\boldsymbol{\Theta}}_1$, we have the following simplified problem:

$$\max_{\widehat{\boldsymbol{v}}_2}\quad \frac{\widehat{\boldsymbol{v}}_2^{\mathrm{H}}\widehat{\boldsymbol{H}}_1\widehat{\boldsymbol{v}}_2}{\widehat{\boldsymbol{v}}_2^{\mathrm{H}}\widehat{\boldsymbol{H}}_2\widehat{\boldsymbol{v}}_2} \tag{62a}$$

$$\text{s.t.}\quad |\widehat{\boldsymbol{v}}_2(i)|=1,\ \forall i=1,2,\ldots,N, \tag{62b}$$

$$\widehat{\boldsymbol{v}}_2(N+1)=1, \tag{62c}$$

where $\widehat{\boldsymbol{v}}_2=[\mathrm{e}^{\mathrm{j}\theta_{2i}},\ldots,\mathrm{e}^{\mathrm{j}\theta_{2N}},1]^{\mathrm{H}}$, $\widehat{\boldsymbol{H}}_1$ is a Hermitian matrix and $\widehat{\boldsymbol{H}}_1=\gamma_s\widehat{\boldsymbol{H}}_{rid}\boldsymbol{A}\boldsymbol{W}_{1r}[\boldsymbol{h}_{sr}+\boldsymbol{H}_{ir}(\overline{\boldsymbol{E}}_K+\beta_1\boldsymbol{E}_K)\widehat{\boldsymbol{\Theta}}_1\boldsymbol{h}_{si}]\{\widehat{\boldsymbol{H}}_{rid}\boldsymbol{A}\boldsymbol{W}_{1r}[\boldsymbol{h}_{sr}+\boldsymbol{H}_{ir}(\overline{\boldsymbol{E}}_K+\beta_1\boldsymbol{E}_K)\widehat{\boldsymbol{\Theta}}_1\boldsymbol{h}_{si}]\}^{\mathrm{H}}$, wherein $\widehat{\boldsymbol{H}}_{rid}=[\mathrm{diag}\{\boldsymbol{h}_{id}^{\mathrm{H}}(\overline{\boldsymbol{E}}_K+\beta_2\boldsymbol{E}_K)\}\cdot\boldsymbol{H}_{ir}^{\mathrm{H}};\boldsymbol{h}_{rd}^{\mathrm{H}}]$. $\widehat{\boldsymbol{H}}_2$ is a positive definite Hermitian matrix and $\widehat{\boldsymbol{H}}_2=\widehat{\boldsymbol{H}}_{rid}\boldsymbol{A}\boldsymbol{W}_{1r}(\beta_1^2\boldsymbol{H}_{ir}\boldsymbol{E}_K\widehat{\boldsymbol{\Theta}}_1\widehat{\boldsymbol{\Theta}}_1^{\mathrm{H}}\boldsymbol{E}_K\boldsymbol{H}_{ir}^{\mathrm{H}}+\boldsymbol{I}_M)\boldsymbol{W}_{1r}^{\mathrm{H}}\boldsymbol{A}^{\mathrm{H}}\widehat{\boldsymbol{H}}_{rid}^{\mathrm{H}}+[\,\beta_2^2\mathrm{diag}\{\boldsymbol{h}_{id}^{\mathrm{H}}\boldsymbol{E}_K\}\mathrm{diag}\{\boldsymbol{E}_K\boldsymbol{h}_{id}\},\ \boldsymbol{0}_{N\times1};\ \boldsymbol{0}_{1\times N},\ 1\,]$. We have the following relaxed transformation:

$$\max_{\widetilde{\boldsymbol{v}}_2}\quad \frac{\widetilde{\boldsymbol{v}}_2^{\mathrm{H}}\widehat{\boldsymbol{H}}_1\widetilde{\boldsymbol{v}}_2}{\widetilde{\boldsymbol{v}}_2^{\mathrm{H}}\widehat{\boldsymbol{H}}_2\widetilde{\boldsymbol{v}}_2} \tag{63a}$$

$$\text{s.t.}\quad \widetilde{\boldsymbol{v}}_2^{\mathrm{H}}\widetilde{\boldsymbol{v}}_2=1, \tag{63b}$$

where $\widetilde{\boldsymbol{v}}_2=\frac{\widehat{\boldsymbol{v}}_2}{\sqrt{N+1}}$. Moreover, in line with GRR theorem, $\widetilde{\boldsymbol{v}}_2$ can be attained as the eigenvector corresponding to the largest eigenvalue of $\widehat{\boldsymbol{H}}_2^{-1}\widehat{\boldsymbol{H}}_1$. Thereby $\widehat{\boldsymbol{v}}_2$ and $\widehat{\boldsymbol{\Theta}}_2$ is achieved.

4.6 Algorithm process and complexity calculation

The proposed LC method WF-GPI-GRR is concluded in Algorithm 3. Its main idea is divided into two parts: the amplifying coefficient of the active element and the iterative idea. The analytic solutions for the amplifying coefficients of the active IRS elements for two-time slots, i.e., β_1 and β_2, are determined by the transmit power of S, AF relay, and IRS. Furthermore, β_1 and β_2 are denoted as (50) and (56). The iterative idea is: fixing $\widehat{\boldsymbol{\Theta}}_1$ and $\widehat{\boldsymbol{\Theta}}_2$, the closed-form expression of $\boldsymbol{A}$ are represented as (57) by MRC-MRT; fixing $\boldsymbol{A}$ and $\widehat{\boldsymbol{\Theta}}_2$, GPI is applied to achieve $\widehat{\boldsymbol{\Theta}}_1$; fixing $\boldsymbol{A}$ and $\widehat{\boldsymbol{\Theta}}_1$, the closed-form expression of $\widehat{\boldsymbol{\Theta}}_2$ is obtained by GRR theorem. Performing the alternative iteration process among $\boldsymbol{A}$, $\widehat{\boldsymbol{\Theta}}_1$, and $\widehat{\boldsymbol{\Theta}}_2$, the maximum system rate is harvested when the convergence condition is met.

In what follows, the computational complexity of the WF-GPI-GRR method is calculated as

$$\begin{aligned}&\mathcal{O}\{D_2(N^3+4M^3+4M^2N+2MN^2+2M^2K+8M^2+6N^2+9MN+5MK+5M+11N+\\&\quad 3+D_3(7N^3+27N^2+43N+18))\}\end{aligned} \tag{64}$$

FLOPs, where D_2 and D_3 respectively denote the iterative numbers for Algorithm 3 and for Algorithm 2. Clearly, the WF-GPI-GRR method has a lower complexity compared with the HP-SDR-FP method.

5 Simulation and discussion

In this section, the rate performance of the proposed two methods, HP-SDR-FP and WF-GPI-GRR, are well evaluated through simulation and numerical results. The three-dimensional locations of S, hybrid

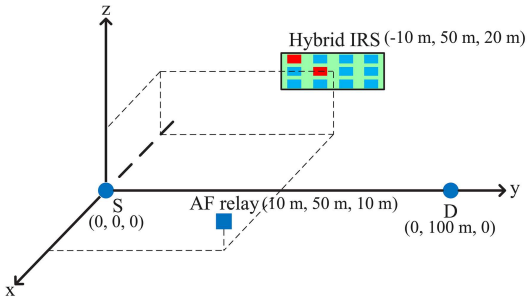

Figure 2 (Color online) Simulation setup.

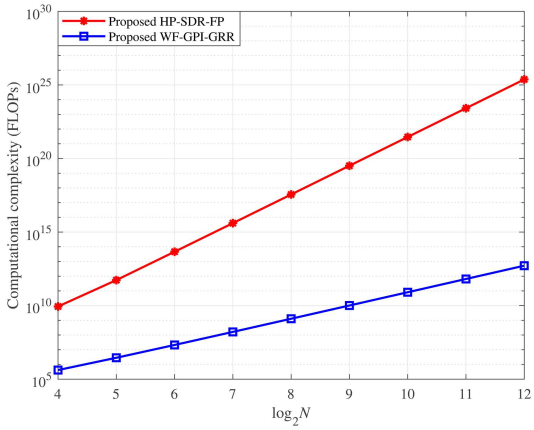

Figure 3 (Color online) Computational complexity of the proposed HP-SDR-FP and WF-GPI-GRR methods versus the number N of hybrid IRS units.

IRS, AF relay, and D are displayed in Figure 2, respectively. The path loss at distance d can be computed in line with the model $\mathrm{PL}(d) = \mathrm{PL}_0 - 10\alpha\log_{10}(\frac{d}{d_0})$, where $\mathrm{PL}_0 = -30$ dB is the path loss at $d_0 = 1$ m and α is the attenuation factor. In this paper, the attenuation factors of S-IRS, IRS-AF relay, S-AF relay, IRS-D, and AF relay-D links are 2.0, 2.0, 3.0, 2.0, and 3.0, respectively. The remaining system parameters are set as follows: $M = 4$, $N = 32$, $K = 16$, $\sigma^2 = -80$ dBm, and the sparse diagonal matrix $\boldsymbol{E}_K$ is randomly generated.

In addition, to better demonstrate the rate gains harvested by the proposed two methods, the following three benchmark schemes need to be considered.

(1) **AF relay + active IRS.** An active IRS-aided AF relay network is considered, and its rate performance is regarded as upper bound.

(2) **AF relay + passive IRS.** An AF relay network aided by a passive IRS is considered, where the IRS only reflects the signal without amplifying the reflected signal.

(3) **AF relay + passive IRS with random phase.** The beamforming matrix $\boldsymbol{A}$ at the AF relay is optimized, while all phase shifts of the IRS elements are randomly generated from (0, 2π].

(4) **Only AF relay.** An AF relay network without IRS is considered, while the AF relay beamforming matrix $\boldsymbol{A}$ is achieved by MRC-MRT, which is given by $\boldsymbol{A} = \sqrt{\frac{P_r}{P_s\|\boldsymbol{\Gamma}\boldsymbol{h}_{sr}\|^2+\sigma^2\|\boldsymbol{\Gamma}\|_F^2}}\boldsymbol{\Gamma}$, where $\boldsymbol{\Gamma} = \frac{\boldsymbol{h}_{rd}\boldsymbol{h}_{sr}^{\mathrm{H}}}{\|\boldsymbol{h}_{rd}^{\mathrm{H}}\|\|\boldsymbol{h}_{sr}\|}$.

In reality, the proposed hybrid IRS-aided AF relay network in this paper gives a general solution for an IRS-assisted AF relay communication network. For instance, when K reduces to zero, it is a case of AF relay+passive IRS. When K is smaller than L, it is a case of AF relay + hybrid IRS. Also, when K is equal to L, it becomes a completely active case.

For a fair comparison, we define that each benchmark scheme has the same total transmit power budget as the proposed AF relay network aided by the hybrid IRS. For instance, the AF relay transmit power budget P_R in the three benchmark schemes is equal to $2P_i + P_r$.

Figure 3 plots the computational complexity versus N. As N increases, the computational complexities of the HP-SDR-FP and WF-GPI-GRR methods increase. Clearly, the proposed WF-GPI-GRR method is LC with highest order $\mathcal{O}(N^3)$ FLOPs, whereas HP-SDR-FP method is with highest order $\mathcal{O}(N^{6.5})$ FLOPs.

Figure 4 demonstrates that the proposed two methods are convergent under different P_s, respectively. Obviously, for the proposed HP-SDR-FP and WF-GPI-GRR methods, it takes five iterations to obtain the maximum rate when $P_s = 10$ dBm, whereas it takes nine iterations to converge to the maximum rate when $P_s = 30$ dBm. Based on the previous two cases, this paper concludes that the proposed two methods are feasible.

Figure 5 depicts the achievable rate versus P_s. It is clear that regardless of the proposed HP-SDR-FP method, WF-GPI-GRR method, and the four comparison benchmarks, their rates can be improved with the increase of P_s. Meanwhile, the rates obtained by the proposed two methods with $(P_i, P_r) = (30$ dBm, 30 dBm) are lower than that of AF relay + active IRS scheme but higher than those of the other three benchmarks with $P_R = 34.77$ dBm. In low power P_s region, the proposed WF-GPI-GRR method obtains

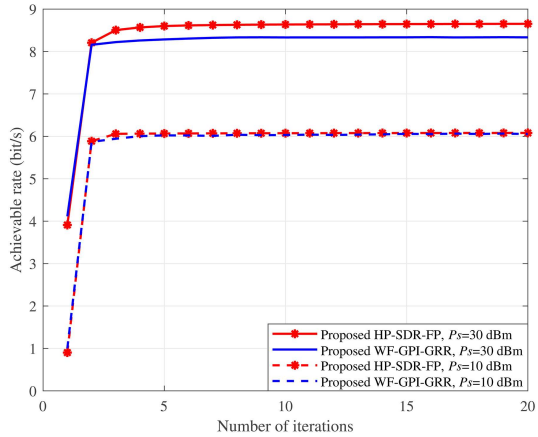

Figure 4 (Color online) Convergence of proposed HP-SDR-FP and WF-GPI-GRR methods with $(M, N, K, P_i, P_r) = (2, 32, 4, 30 \text{ dBm}, 30 \text{ dBm})$.

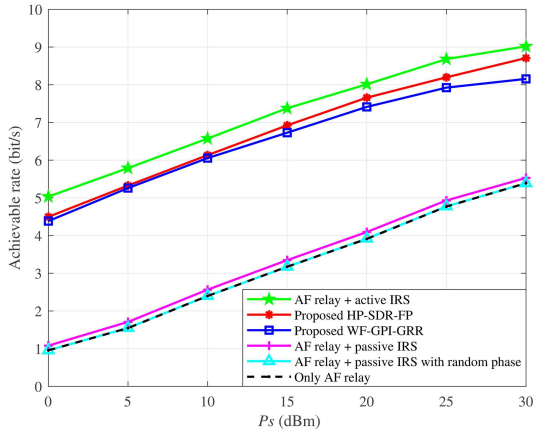

Figure 5 (Color online) Achievable rate versus the transmit power P_s at S with $(M, N, K) = (4, 32, 16)$.

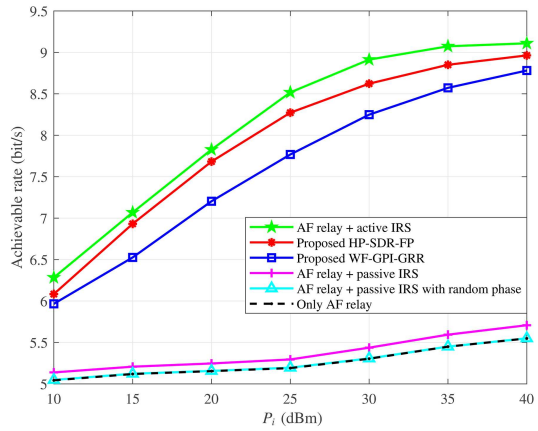

Figure 6 (Color online) Achievable rate versus the transmit power P_i at hybrid IRS with $(M, N, K, P_s, P_r, P_R) = (4, 32, 16, 30 \text{ dBm}, 30 \text{ dBm}, 34.77 \text{ dBm})$.

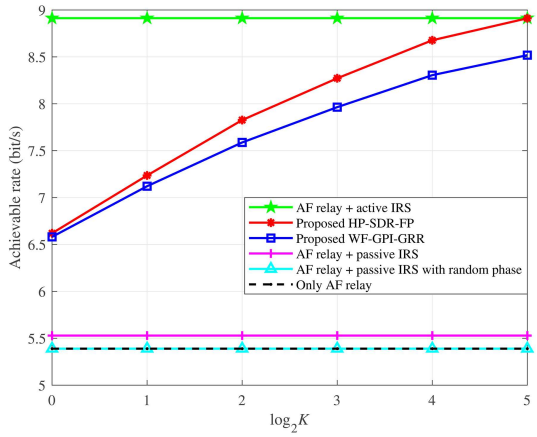

Figure 7 (Color online) Achievable rate versus the number K of active IRS units with $(M, N, P_s, P_i, P_r, P_R) = (4, 32, 30 \text{ dBm}, 30 \text{ dBm}, 30 \text{ dBm}, 34.77 \text{ dBm})$.

slightly lower rate performance than the HP-SDR-FP method. Compared with AF relay + active IRS benchmarks, the proposed two methods can respectively obtain 139.06% and 136.06% rate gains when $P_s = 10$ dBm.

Figure 6 shows the achievable rate versus P_i. In the case of $(P_r, P_R) = (30 \text{ dBm}, 34.77 \text{ dBm})$, it is observed that the proposed HP-SDR-FP and WF-GPI-GRR methods can achieve significant rate improvement compared with the three benchmarks: AF relay + passive IRS, AF relay + passive IRS with random phase, and Only AF relay. Meanwhile, the benchmark called AF + active IRS achieves the highest rate performance. In all P_i regions, the HP-SDR-FP method is significantly superior to the WF-GPI-GRR method. For example, when P_i is equal to 40 dBm, the proposed HP-SDR-FP and WF-GPI-GRR methods can respectively harvest up to about 3.3-bit and 3.1-bit rate gains over AF relay + passive IRS.

Figure 7 presents the achievable rate versus K. Obviously, as K increases, the rate gains obtained by the proposed two methods with $(P_i, P_r) = (30 \text{ dBm}, 30 \text{ dBm})$ gradually increase and become more significant over the three benchmark schemes with $P_R = 34.77$ dBm. In addition, when K varies from 1 to 32, the rate gap between the proposed two methods and AF relay + active IRS reduces. In particular, when $K = 32$, the rate attained by the HP-SDR-FP method approaches that of AF relay + active IRS. In Figure 7, it is presented that the HP-SDR-FP and WF-GPI-GRR methods perform much better than AF relay + passive IRS, which shows that the optimization of beamforming is important and efficient.

6 Conclusion

To address the problem of maximizing the rate of the proposed AF relay wireless network aided by hybrid IRS, an HP-SDR-FP method has been first proposed to alternately design the beamforming matrix and reflecting coefficient matrices of two-time slots. However, the optimization process of the HP-SDR-FP method resulted in high computational complexity. With the aim of reducing the computational complexity, an LC WF-GPI-GRR method has been put forward. Simulation results have demonstrated that the rates of the HP-SDR-FP and WF-GPI-GRR methods are lower, about 0.5 bit, than that of AF relay + active IRS. However, the proposed methods can achieve appreciable rate gains over the other three benchmarks, which verified that the serious path loss caused by passive IRS can be weakened by introducing active IRS. Furthermore, it is validated that the HP-SDR-FP method is superior to the WF-GPI-GRR method.

Acknowledgements This work was supported in part by National Natural Science Foundation of China (Grant Nos. U22A2002, 62071234), Hainan Province Science and Technology Special Fund (Grant No. ZDKJ2021022), Scientific Research Fund Project of Hainan University (Grant No. KYQD(ZR)-21008), and Collaborative Innovation Center of Information Technology, Hainan University (Grant No. XTCX2022XXC07).

References

1 Chettri L, Bera R. A comprehensive survey on Internet of Things (IoT) toward 5G wireless systems. IEEE Int Things J, 2020, 7: 16–32
2 Chen J, Li S, Xing J, et al. Multiple nodes access of wireless beam modulation for 6G-enabled Internet of Things. IEEE Int Things J, 2021, 8: 15191–15204
3 Wong V W S, Schober R, Ng D W K, et al. Multiple Nodes Access of Wireless Beam Modulation for 6G-enabled Internet of Things. Cambridge: Cambridge University Press, 2017
4 Zhang Y, Cheng W, Zhang W. Multiple access integrated adaptive finite blocklength for ultra-low delay in 6G wireless networks. IEEE Trans Wireless Commun, 2024, 23: 1670–1683
5 Fu Y, Cheng W, Zhang W, et al. Scalable extraction based semantic communication for 6G wireless networks. IEEE Commun Mag, 2024, 62: 96–102
6 Poursajadi S, Madani M H, Bizaki H K. Power allocation and outage probability analysis of AF relaying systems with multiple antennas at terminal node. IEEE Trans Veh Technol, 2017, 66: 377–384
7 Zou Y, Champagne B, Zhu W P, et al. Relay-selection improves the security-reliability trade-off in cognitive radio systems. IEEE Trans Commun, 2015, 63: 215–228
8 Pang X, Zhao N, Tang J, et al. IRS-assisted secure UAV transmission via joint trajectory and beamforming design. IEEE Trans Commun, 2022, 70: 1140–1152
9 Wu Q, Zhang R. Beamforming optimization for wireless network aided by intelligent reflecting surface with discrete phase shifts. IEEE Trans Commun, 2020, 68: 1838–1851
10 Liang Y C, Chen J, Long R Z, et al. Reconfigurable intelligent surfaces for smart wireless environments: channel estimation, system design and applications in 6G networks. Sci China Inf Sci, 2021, 64: 200301
11 Tang W, Chen M Z, Chen X, et al. Wireless communications with reconfigurable intelligent surface: path loss modeling and experimental measurement. IEEE Trans Wireless Commun, 2021, 20: 421–439
12 Yang L, Yan X, da Costa D B, et al. Indoor mixed dual-hop VLC/RF systems through reconfigurable intelligent surfaces. IEEE Wireless Commun Lett, 2020, 9: 1995–1999
13 Tao Q, Zhang S W, Zhong C J, et al. Joint information transmission design for intelligent reflecting surface aided system with discrete phase shifts. Sci China Inf Sci, 2023, 66: 132303
14 Wu Q, Zhou X, Chen W, et al. IRS-aided WPCNs: a new optimization framework for dynamic IRS beamforming. IEEE Trans Wireless Commun, 2022, 21: 4725–4739
15 Cao H, Li Z, Chen W. Resource allocation for IRS-assisted wireless powered communication networks. IEEE Wireless Commun Lett, 2021, 10: 2450–2454
16 Shi W, Wu Q, Xiao F, et al. Secrecy throughput maximization for IRS-aided MIMO wireless powered communication networks. IEEE Trans Commun, 2022, 70: 7520–7535
17 Pan C, Ren H, Wang K, et al. Multicell MIMO communications relying on intelligent reflecting surfaces. IEEE Trans Wireless Commun, 2020, 19: 5218–5233
18 Rezaei A, Khalili A, Jalali J, et al. Energy-efficient resource allocation and antenna selection for IRS-assisted multicell downlink networks. IEEE Wireless Commun Lett, 2022, 11: 1229–1233
19 Zhou X, Yan S, Wu Q, et al. Intelligent reflecting surface (IRS)-aided covert wireless communications with delay constraint. IEEE Trans Wireless Commun, 2022, 21: 532–547
20 Chen X, Zheng T X, Dong L, et al. Enhancing MIMO covert communications via intelligent reflecting surface. IEEE Wireless Commun Lett, 2022, 11: 33–37
21 Wu Q, Zhang R. Weighted sum power maximization for intelligent reflecting surface aided SWIPT. IEEE Wireless Commun Lett, 2020, 9: 586–590
22 Shi W, Zhou X, Jia L, et al. Enhanced secure wireless information and power transfer via intelligent reflecting surface. IEEE Commun Lett, 2021, 25: 1084–1088
23 Shu F, Yang L, Jiang X, et al. Beamforming and transmit power design for intelligent reconfigurable surface-aided secure spatial modulation. IEEE J Sel Top Signal Process, 2022, 16: 933–949
24 Shu F, Teng Y, Li J, et al. Enhanced secrecy rate maximization for directional modulation networks via IRS. IEEE Trans Commun, 2021, 69: 8388–8401
25 Shen H, Xu W, Gong S, et al. Secrecy rate maximization for intelligent reflecting surface assisted multi-antenna communications. IEEE Commun Lett, 2019, 23: 1488–1492
26 Shi W P, Pan C H, Shu F, et al. Weighted sum power maximization for STAR-RIS-aided SWIPT systems with nonlinear energy harvesting. Sci China Inf Sci, 2024, 67: 202301
27 Zou Y, Wang X, Shen W. Optimal relay selection for physical-layer security in cooperative wireless networks. IEEE J Sel Areas Commun, 2013, 31: 2099–2111
28 Rankov B, Wittneben A. Spectral efficient protocols for half-duplex fading relay channels. IEEE J Sel Areas Commun, 2007, 25: 379–389

29 Wang W, Liu X, Tang J, et al. Beamforming and jamming optimization for IRS-aided secure NOMA networks. IEEE Trans Wireless Commun, 2022, 21: 1557–1569
30 Hua M, Wu Q. Joint dynamic passive beamforming and resource allocation for IRS-aided full-duplex WPCN. IEEE Trans Wireless Commun, 2022, 21: 4829–4843
31 Yang L, Guo W, Ansari I S. Mixed dual-hop FSO-RF communication systems through reconfigurable intelligent surface. IEEE Commun Lett, 2020, 24: 1558–1562
32 Yildirim I, Kilinc F, Basar E, et al. Hybrid RIS-empowered reflection and decode-and-forward relaying for coverage extension. IEEE Commun Lett, 2021, 25: 1692–1696
33 Wang X, Shu F, Shi W, et al. Beamforming design for IRS-aided decode-and-forward relay wireless network. IEEE Trans Green Commun Netw, 2022, 6: 198–207
34 Abdullah Z, Chen G, Lambotharan S, et al. A hybrid relay and intelligent reflecting surface network and its ergodic performance analysis. IEEE Wireless Commun Lett, 2020, 9: 1653–1657
35 Nguyen N T, Vu Q D, Lee K, et al. Spectral efficiency optimization for hybrid relay-reflecting intelligent surface. In: Proceedings IEEE International Conference on Communications Workshops (ICC Workshops), 2021
36 Obeed M, Chaaban A. Relay-reconfigurable intelligent surface cooperation for energy-efficient multiuser systems. In: Proceedings of IEEE International Conference on Communications Workshops (ICC Workshops), 2021
37 Zhang Z J, Dai L L, Chen X B, et al. Active RIS vs. passive RIS: which will prevail in 6G? IEEE Trans Commun, 2023, 71: 1707–1725
38 Zhi K, Pan C H, Ren H, et al. Active RIS versus passive RIS: which is superior with the same power budget? IEEE Commun Lett, 2022, 26: 1150–1154
39 Dong L, Wang H M, Bai J. Active reconfigurable intelligent surface aided secure transmission. IEEE Trans Veh Technol, 2022, 71: 2181–2186
40 Peng Z J, Liu X Y, Liu X, et al. Performance analysis of active RIS-aided multi-pair full-duplex communications with spatial correlation and imperfect CSI. Sci China Inf Sci, 2023, 66: 192304
41 Zhou X, Li J, Shu F, et al. Secure SWIPT for directional modulation-aided AF relaying networks. IEEE J Sel Areas Commun, 2019, 37: 253–268
42 Mensi N, Rawat D B. Reconfigurable intelligent surface selection for wireless vehicular communications. IEEE Wireless Commun Lett, 2022, 11: 1743–1747